

Circular strings, magnons, plane waves and local quenches in BTZ

Justin R. David^a Rahul Metya^b

^a*Centre for High Energy Physics, Indian Institute of Science, C. V. Raman Avenue, Bangalore 560012, India.*

^b*International Centre for Theoretical Sciences-TIFR, Shivakote, Heseraghatta Hobli, Bangalore North 560089, India.*

E-mail: justin@iisc.ac.in, rahul.metya@icts.res.in

ABSTRACT: We show that string theory on the geometry $BTZ \times S^3 \times M$ supported with either Neveu-Schwarz flux or Ramond flux admits states which obey identical dispersion relations to those of classical solutions like circular strings, giant magnons, or plane wave excitations in the geometry $AdS_3 \times S^3 \times M$. Here, M can be T^4 , $K3$, or $S^3 \times S^1$. This is made possible by the map, which takes the particle at the origin of AdS_3 with angular momentum along one of the angles of S_3 to a particle falling into the BTZ horizon. We use this map to construct circular strings, magnons, as well as plane waves in the BTZ geometry. We show that the $SL(2, R)$ charges of these states on AdS_3 and that of the corresponding states in the BTZ geometry are related by a boost. The dual description of these states in the BTZ geometry are local quench in the thermal CFT. These quenches carry energy density, R -charges, non-trivial expectation value of the marginal operator dual to the dilaton and move on the light cone in CFT. In general, the left and the right moving quenches are not symmetric.

Contents

1	Introduction	1
2	Geodesics and their charges	3
2.1	The in-falling particle in BTZ	4
2.2	In-falling particle with longitudinal velocity	9
3	In-falling classical strings in BTZ	13
4	Plane wave spectra in BTZ	18
4.1	The Penrose limit of $BTZ \times S^3 \times S^3 \times S^1$	19
5	In-falling strings as local quenches	26
5.1	CFT duals of geodesics solutions in $AdS_3 \times S^3 \times M$	28
5.2	In falling spinning geodesics in $BTZ \times S^3 \times M$ as quenches	34
5.3	Quenches dual to the circular string	42
6	Conclusions	43
A	Penrose limit of Schwarzschild black hole in $AdS_5 \times S^5$	44

1 Introduction

The BTZ black hole [1, 2] It is one of the most well-studied solutions among black hole geometries. It also occurs as the near-horizon geometry of the $D1D5$ black hole in string theory [3]. It serves as a prototype for studies of black hole entropy, information paradox, and the holographic dual of large c CFTs at finite temperature. This is partly because many aspects of the BTZ black hole are exactly solvable. Solutions for geodesics, wave equations of arbitrary spin fields [4, 5] can be obtained in closed form as it is locally AdS_3 . String propagation has also been studied earlier using the WZW model of the BTZ geometry. [6–11]. However, a clear physical interpretation of the states of the string is lacking. This is important due to the existence of the horizon. Clearly, there must be string states that fall into the horizon, and these have not been identified and studied in earlier work.

In this paper, we identify string states that fall into the horizon of the BTZ black hole. The background we consider is string theory on $BTZ \times S^3 \times M$, where M can be T^4 , $K3$, or $S^3 \times S^1$. A class of states that play an important role in discussions of integrability in the AdS backgrounds are giant magnons, circular strings, and the plane wave spectra. The construction of all these states for the AdS_3 background begins with a geodesic at the origin of AdS_3 . For instance, the plane wave spectra are obtained by zooming into the geometry around the BPS geodesic at the origin of AdS_3 with angular momentum along

one of the angles of the S^3 [12]. This geodesic is light-like when considered on $AdS_3 \times S^3$, but time-like when considered only on AdS_3 . There exists a map that relates the time-like geodesic at the origin in AdS_3 to an in-falling geodesic in BTZ [13]. To be explicit, this map is given by the following relations

$$\begin{aligned} X_0 &= \sqrt{r^2 + R^2} \sin t = \frac{R}{M} \sqrt{\rho^2 - M^2} \sinh M\tau, \\ X_1 &= \sqrt{r^2 + R^2} \cos t = \frac{R}{M} \left[\sqrt{\rho^2 - M^2} \sinh \eta_1 \cosh M\tau + \rho \cosh \eta_1 \cosh Mx \right], \\ X_2 &= r \sin \phi = \frac{R}{M} \rho \sinh Mx, \\ X_3 &= r \cos \phi = \frac{R}{M} \left[\sqrt{\rho^2 - M^2} \cosh \eta_1 \cosh M\tau + \rho \sinh \eta_1 \cosh Mx \right]. \end{aligned} \quad (1.1)$$

Note that the embedding coordinates satisfy

$$-X_0^2 - X_1^2 + X_2^2 + X_3^2 = -R^2, \quad (1.2)$$

where R is the radius of AdS_3 . The induced metric in the t, r, ϕ coordinates is global AdS_3 , and in the τ, ρ, x coordinates is BTZ, M is the location of the horizon. It can be seen that this map relates the particle at the origin $r = 0$ to that of a geodesic in-falling into the BTZ horizon. This map depends on the parameter η_1 , which can be related to the position of the particle when it is released in the BTZ geometry. We use this map and its generalisation, which allows us to give velocity along the x direction to construct and study giant magnons and circular strings in BTZ.

The classical solutions in the WZW sigma model of the BTZ background carry conserved $SL(2, R)$ charges. We evaluate these charges and show that they are related to the charges of the corresponding solution in AdS_3 by a $SO(1, 2)$ boost. This boost parameter depends on the map relating geodesics in AdS_3 and BTZ and for the map given in (1.1) it turns out to be η_1 . The resulting solutions in BTZ obey the same dispersion relation as that of the solution in AdS_3 . This is because the dispersion relation results from the Virasoro condition, which relates the $SL(2, R)$ and the $SU(2)$ Casimirs. The $SL(2, R)$ Casimir remains invariant under the $SO(1, 2)$ boosts and therefore the Virasoro condition and consequently the dispersion relation is BTZ and AdS_3 are identical.

We then study the plane wave spectrum in the BTZ geometry. Recall in $AdS_3 \times S^3$, The plane wave limit and its spectrum of string states are obtained by zooming into the geometry near a lightlike geodesic. This particle sits at the origin in AdS_3 and spins along one of the isometries of S^3 . We use the map (1.1) and its generalisation, which relates the time-like geodesic at the origin in AdS_3 to an in-falling geodesic in BTZ with angular momentum along one of the circles of S^3 , to zoom into this geometry of the BTZ. Plane wave limits of in-falling geodesics into black hole horizons have been studied earlier, see for example in [14], the resulting metric depends on the light cone co-ordinate. The limit we obtain by zooming in near in-falling geodesics to the BTZ horizon with angular momentum on S^3 results in a homogeneous plane wave metric. In fact, the plane wave dispersion relation in the BTZ geometry is identical to that of the AdS_3 case, which reflects

the local AdS_3 nature of the BTZ geometry, and it does not depend on the parameters of the map.

Finally, we examine the interpretation of the states that we have found in the BTZ geometry. These states should be excitations of the thermal state of the corresponding boundary CFT. The boundary CFT in this case is the symmetric product CFT on T^4 or $K3$, or in the case $S^3 \times S^1$, it is the instanton moduli space on $S^3 \times S^1$. We show that the classical states in the bulk, geodesics, circular strings, and magnons are dual to local quenches similar to that studied in [15] for the 3 dimensional BTZ geometry which carry only energy density and move on the light cone in the CFT. Here, however, the quenches in addition to energy density carry R charges which arise due to the angular momentum on S^3 . These states also have a non-trivial expectation value of the marginal operator dual to the dilaton in the CFT. We show that for the more general case of the map in (1.1), which allows transverse velocity of the in-falling particle in the x direction, the dual quenches on the left and right light cones are not symmetric, and the amplitude of the pulse differs. Thus, these quenches generalise those found first in [15]. The figure 1 shows the plot of the energy density of these quenches, which clearly shows the asymmetric left and right moving pulses travelling at the speed of light.

The organisation of this paper is as follows. In section 2, we study the map which relates the time-like geodesic of a particle at the origin of global AdS to that of an in-falling particle in BTZ in detail, and its generalisation. By examining the WZW sigma model on global AdS and that of BTZ , we show that the conserved charges of the geodesics in each of the spaces are related by an $SO(1, 2)$ transformation. In section 3, we zoom into the geometry of the in-falling geodesic in BTZ and show that the geometry reduces to that of a homogeneous plane with identical to that in AdS_3 . In section 5, we derive the description of the in-falling classical solutions in the BTZ geometry as local quenches in the thermal 2-dimensional CFT. Section 6 has our conclusions. Appendix A reviews the Penrose limits of the Schwarzschild black hole in $AdS_5 \times S^5$.

2 Geodesics and their charges

AdS_3 and BTZ spacetime are locally isomorphic. In fact, the metric of both the space times can be constructed by different parametrisations of the hyperboloid

$$-X_0^2 - X_1^2 + X_2^2 + X_3^2 = -R^2. \quad (2.1)$$

Let us recall how this comes about, consider the embeddings

$$\begin{aligned} X_0 &= \sqrt{r^2 + R^2} \sin t = \frac{R}{M} \sqrt{\rho^2 - M^2} \sinh M\tau, \\ X_1 &= \sqrt{r^2 + R^2} \cos t = \frac{R}{M} \rho \cosh Mx, \\ X_2 &= r \sin \phi = \frac{R}{M} \rho \sinh Mx, \\ X_3 &= r \cos \phi = \frac{R}{M} \sqrt{\rho^2 - M^2} \cosh M\tau. \end{aligned} \quad (2.2)$$

The induced metric on the hyperboloid in the t, r, ϕ coordinates is that of AdS_3

$$ds_{AdS_3}^2 = -(r^2 + R^2)dt^2 + \frac{R^2}{r^2 + R^2}dr^2 + r^2d\phi^2. \quad (2.3)$$

It is understood that we need to think of t as the coordinate on the covering space in global AdS_3 . In the τ, ρ, x coordinates, the metric is given by

$$ds_{BTZ}^2 = R^2 \left[-(\rho^2 - M^2)d\tau^2 + \frac{d\rho^2}{\rho^2 - M^2} + \rho^2dx^2 \right]. \quad (2.4)$$

The radius of curvature of both the spaces is set by R , while the location of the horizon in BTZ is given by M . Note that we obtain the Rindler BTZ metric with a planar horizon, identifying $Rx \sim Rx + 2\pi$ results in the BTZ black hole with a circular horizon. We will work with the Rindler BTZ in this paper. The map between AdS_3 and BTZ coordinates given in (2.2) allows us to relate geodesics in these spaces. We will exploit this fact to construct classical string solutions in BTZ as well as to identify the geodesics we need to zoom in to obtain the plane wave limit. We can choose to embed BTZ in the hyperboloid differently. For example, we can introduce a boost between the parametrisation of X_1 and X_3 in the BTZ embedding (2.2), and still obtain the metric of the BTZ. With this boost, the map becomes

2.1 The in-falling particle in BTZ

Consider the following coordinate transformation

$$\begin{aligned} X_0 &= \sqrt{r^2 + R^2} \sin t = \frac{R}{M} \sqrt{\rho^2 - M^2} \sinh M\tau, \\ X_1 &= \sqrt{r^2 + R^2} \cos t = \frac{R}{M} \left[-\sqrt{\rho^2 - M^2} \sinh \eta_1 \cosh M\tau + \rho \cosh \eta_1 \cosh Mx \right], \\ X_2 &= r \sin \phi = \frac{R}{M} \rho \sinh Mx, \\ X_3 &= r \cos \phi = \frac{R}{M} \left[\sqrt{\rho^2 - M^2} \cosh \eta_1 \cosh M\tau - \rho \sinh \eta_1 \cosh Mx \right]. \end{aligned} \quad (2.5)$$

Note that the induced metric in the τ, ρ, x coordinate still remains BTZ. Given the map (2.5) between AdS_3 and BTZ, let us examine the trajectory of a time-like geodesic at the origin of AdS_3 in BTZ. The geodesic in AdS_3 is given by

$$t = \kappa \sigma^0, \quad r(\sigma^0) = 0, \quad \phi(\sigma^0) = 0. \quad (2.6)$$

From the map in (2.5), we see that the BTZ co-ordinates on this trajectory must satisfy

$$\sqrt{\rho^2 - M^2} \cosh \eta_1 \cosh M\tau - \rho \sinh \eta_1 = 0, \quad x = 0. \quad (2.7)$$

Here, it is understood that τ, ρ are functions of the affine parameter σ^0 . Now, from the first 2 equations (2.5), we obtain the relations

$$\begin{aligned} R \sin t &= \frac{R}{M} \sqrt{\rho^2 - M^2} \sinh M\tau, \\ R \cos t &= \frac{R}{M} \frac{\rho}{\cosh \eta_1}. \end{aligned} \quad (2.8)$$

Here we have used $r = 0$ and the relation (2.7) to obtain the second line. Differentiating (2.7) with respect to σ^0 , we obtain

$$\dot{\tau} \cosh \eta_1 \sinh M\tau = -\frac{M\dot{\rho}}{(\rho^2 - M^2)^{\frac{3}{2}}} \sinh \eta_1. \quad (2.9)$$

Similarly differentiating the first equation of (2.8), we obtain

$$\begin{aligned} R\kappa \cos t &= \frac{R}{M} \left(\frac{\rho\dot{\rho}}{\sqrt{\rho^2 - M^2}} \sinh M\tau + M\dot{\tau} \sqrt{\rho^2 - M^2} \cosh M\tau \right), \\ &= \frac{R}{M} \frac{\rho\kappa}{\cosh \eta_1}. \end{aligned} \quad (2.10)$$

Here we have used the trajectory $t = \kappa\sigma^0$ in AdS_3 . Now using (2.9) and (2.7) to eliminate $\dot{\rho}$ and τ , we obtain the relation

$$(\rho^2 - M^2)\dot{\tau} = \kappa M \sinh \eta_1. \quad (2.11)$$

Substituting this relation and eliminating the dependence on τ in (2.9), we obtain

$$-\frac{M^2\kappa^2 \sinh^2 \eta_1}{\rho^2 - M^2} + \frac{\dot{\rho}^2}{\rho^2 - M^2} = -\kappa^2. \quad (2.12)$$

Comparison with the in-falling geodesic in BTZ

Consider time like geodesic equations in the BTZ metric given in (2.4). The isometry along the τ and x direction leads to the following conserved quantities

$$-R^2(\rho^2 - M^2)\dot{\tau} = E, \quad R^2\rho^2\dot{x} = v. \quad (2.13)$$

The condition that the geodesic is time-like with mass \tilde{m} leads to the equation

$$-R^2(\rho^2 - M^2)\dot{\tau}^2 + R^2 \frac{\dot{\rho}^2}{\rho^2 - M^2} + R^2\rho^2\dot{x}^2 = -\tilde{m}^2. \quad (2.14)$$

We can eliminate $\dot{\tau}, \dot{x}$ using the constants of motion (2.13) and obtain

$$-\frac{E^2}{R^4(\rho^2 - M^2)} + \frac{\dot{\rho}^2}{\rho^2 - M^2} + \frac{v^2}{R^4\rho^2} = -\frac{\tilde{m}^2}{R^2}. \quad (2.15)$$

Comparison of these equations with the equation of the trajectory obtained in (2.11) and (2.12), we can identify it as the in-falling geodesic with the following constants of motion

$$\frac{E}{R^2} = -\kappa M \sinh \eta_1, \quad v = 0, \quad \frac{\tilde{m}^2}{R^2} = \kappa^2. \quad (2.16)$$

Once this map is made, the boost parameter η_1 can be related to the point of the release of the particle from (2.12). We see that $\dot{\rho} = 0$ at

$$\rho|_{\dot{\rho}=0} = M \cosh \eta_1. \quad (2.17)$$

Therefore, we have concluded that the map (2.5) takes the time-like geodesic at the centre of AdS_3 to a radially in-falling geodesic in BTZ released at radial distance $M \cosh \eta_1$. The initial conditions of this geodesic at $\sigma^0 = 0$ are

$$\begin{aligned} x(0) = 0, \quad \dot{x}(0) = 0, \quad \tau(0) = 0, \quad \dot{\tau}(0) &= \frac{\kappa}{M \sinh \eta_1}, \\ \rho(0) = M \cosh \eta_1, \quad \dot{\rho} &= 0. \end{aligned} \quad (2.18)$$

This can be seen by using the equations (2.13), (2.16), (2.17) and (2.8) at $\sigma^0 = 0$.

$SL(2, R)$ charges of the in-falling particle

The geodesics both in AdS_3 and BTZ are solutions to the string sigma model on $AdS_3 \times S^3 \times M$ or $BTZ \times S^3 \times M$. Let us describe the bosonic part of the sigma model on AdS_3 or BTZ by the $SL(2, R)$ WZW action

$$\begin{aligned} S &= S_{SL(2,R)} + S_{SU(2)} + S_M, \\ S_{SL(2,R)} &= -\frac{k}{8\pi} \int_{\Sigma} d^2\sigma \operatorname{Tr} [g^{-1} \partial_a g \ g^{-1} \partial^a g] + \frac{k}{12\pi} q \int_{\mathcal{B}} \operatorname{Tr} [g^{-1} dg \wedge g^{-1} dg \wedge g^{-1} dg]. \end{aligned} \quad (2.19)$$

Here $S_{SU(2)}$ refers to the $SU(2)$ WZW model on S^3 and S_M refers to the sigma model on M . For the present, let us focus on the $SL(2, R)$ WZW model. The level k is related to the radius of AdS_3 or BTZ by $\alpha' k = R^2$. The parameter q in front of the topological term lies between $0 \leq q \leq 1$. When $q = 0$, the background is supported by pure Ramond flux, and when $q = 1$, the model contains pure Neveu-Schwarz flux. The index a runs over the world sheet co-ordinates σ^0, σ^1 with the signature $(-1, 1)$. The world sheet space coordinate σ^1 runs from 0 to 2π when describing closed strings. Σ is the world sheet, which is the boundary of the 3-manifold \mathcal{B} . The $SL(2, R)$ model can be used to describe both AdS_3 and BTZ by appropriate parametrisation of the group element g . In terms of the embedding coordinates, g is given by

$$g = \frac{1}{R} \begin{pmatrix} X_1 + X_2 & X_3 + X_0 \\ X_3 - X_0 & X_1 - X_2 \end{pmatrix}, \quad -X_0^2 - X_1^2 + X_2^2 + X_3^2 = -R^2. \quad (2.20)$$

To describe string propagation on the global AdS_3 , we choose the embedding as in [8].

$$\begin{aligned} X_0 &= \sqrt{r^2 + R^2} \sin t, & X_1 &= \sqrt{r^2 + R^2} \cos t, \\ X_2 &= r \sin \phi, & X_3 &= r \cos \phi. \end{aligned} \quad (2.21)$$

On the other hand, to describe string propagation in BTZ, we choose the embedding [10].

$$\begin{aligned} X_0 &= \frac{R}{M} \sqrt{\rho^2 - M^2} \sinh M\tau, & X_1 &= \frac{R}{M} \rho \cosh Mx, \\ X_2 &= \frac{R}{M} \rho \sinh Mx, & X_3 &= \frac{R}{M} \sqrt{\rho^2 - M^2} \cosh M\tau. \end{aligned} \quad (2.22)$$

The sigma model exhibits left and right $SL(2, R)$ conserved charges whose expressions are given by

$$Q_L = \frac{1}{2\pi} \int_0^{2\pi} d\sigma^1 \left(g^{-1} \dot{g} + q g^{-1} g' \right), \quad Q_R = \frac{1}{2\pi} \int_0^{2\pi} d\sigma^1 \left(\dot{g} g^{-1} - q g' g^{-1} \right). \quad (2.23)$$

Here \dot{g} refers to derivative with the world sheet time coordinate σ^0 and g' refers to derivative with the world sheet space coordinate σ^1 . Since $g \in SL(2, R)$, these charges belong to the Lie algebra of $SL(2, R)$ and we can project them along its 3 generators as follows

$$Q_{L,R}^{(i)} = i \operatorname{Tr} [\Sigma^i Q_{L,R}], \quad (2.24)$$

where the Σ 's are related to the Pauli matrices $\hat{\sigma}_i$ as

$$\Sigma^1 = \frac{i}{2} \hat{\sigma}_1, \quad \Sigma^2 = \frac{i}{2} \hat{\sigma}_3, \quad \Sigma^3 = -\frac{1}{2} \hat{\sigma}_2. \quad (2.25)$$

Let us evaluate the $SL(2, R)$ charges on the time like a geodesic sitting at the origin described by the trajectory (2.6). Note that for geodesics, the contribution proportional to q in the charges (2.23) vanishes. The left and right $SL(2, R)$ charges for this geodesic are given by

$$Q_{L,R}^{(1)}|_{AdS_3} = 0, \quad Q_{L,R}^{(2)}|_{AdS_3} = 0, \quad Q_{L,R}^{(3)}|_{AdS_3} = \kappa \quad (2.26)$$

We proceed with the evaluation of the charges of the in-falling geodesic in BTZ related to a time-like particle at the origin of AdS_3 by the map in (2.5). For this, let us substitute the embedding (2.22) into g and evaluate the charges. For the left $SL(2, R)$ charges, we obtain

$$\begin{aligned} Q_L^{(1)} &= -\frac{\dot{\rho}}{\sqrt{\rho^2 - M^2}} \cosh M(\tau - x) - \frac{(\dot{x} + \dot{\tau})}{M} \rho \sqrt{\rho^2 - M^2} \sinh M(\tau - x), \\ Q_L^{(2)} &= \frac{M^2 - \rho^2}{M} \dot{\tau} - \frac{\rho^2}{M} \dot{x}, \\ Q_L^{(3)} &= \frac{\dot{\rho}}{\sqrt{\rho^2 - M^2}} \sinh M(\tau - x) + \frac{(\dot{x} + \dot{\tau})}{M} \rho \sqrt{\rho^2 - M^2} \cosh M(\tau - x). \end{aligned} \quad (2.27)$$

Since these charges are constants of motion, we can evaluate them by substituting the initial conditions (2.18) for the in-falling particle. We find that the charges are given by

$$Q_L^{(1)}|_{BTZ} = 0, \quad Q_L^{(2)}|_{BTZ} = -\kappa \sinh \eta_1, \quad Q_L^{(3)}|_{BTZ} = \kappa \cosh \eta_1 \quad (2.28)$$

Now, comparing the charges of the time like geodesic at the origin (2.26) to that of the in-falling particle in BTZ, we find that

$$\begin{pmatrix} Q_L^{(1)} \\ Q_L^{(2)} \\ Q_L^{(3)} \end{pmatrix}_{BTZ} = \begin{pmatrix} 1 & 0 & 0 \\ 0 & \cosh \eta_1 & -\sinh \eta_1 \\ 0 & -\sin \eta_1 & \cosh \eta_1 \end{pmatrix} \begin{pmatrix} Q_L^{(1)} \\ Q_L^{(2)} \\ Q_L^{(3)} \end{pmatrix}_{AdS_3}. \quad (2.29)$$

Therefore, the charges of the in-falling particle in BTZ, which is obtained from the time-like particle at the centre of AdS_3 by the map, are related by an $SO(1, 2)$ boost. There is another way to see that the charges of the geodesics of interest are related by boosts.

From the map in (2.5), We see that on the geodesic, we have the relation

$$\begin{aligned} X_0 &= R \sin t = \frac{R}{M} \sqrt{\rho^2 - M^2} \sinh M\tau, \\ X_1 \cosh \eta_1 + X_3 \sinh \eta_1 &= R \cos t \cosh \eta_1 = \frac{R}{M} \rho \cosh Mx|_{x=0}, \\ X_2 &= 0 = \frac{R}{M} \rho \sinh Mx|_{x=0} \\ X_3 \cos \eta_1 + X_1 \sinh \eta_1 &= +R \cos t \sinh \eta_1 = \frac{R}{M} \sqrt{\rho^2 - M^2} \cosh M\tau \end{aligned} \quad (2.30)$$

From this, we see that evaluating the charges for the geodesics in the BTZ embedding can be done by relating the $SL(2, R)$ element along the geodesic in BTZ to that of AdS_3 as follows as on the geodesic

$$g_{BTZ} = \begin{pmatrix} \cosh \frac{\eta_1}{2} & \sinh \frac{\eta_1}{2} \\ \sinh \frac{\eta_1}{2} & \cosh \frac{\eta_1}{2} \end{pmatrix} g_{AdS_3} \begin{pmatrix} \cosh \frac{\eta_1}{2} & \sinh \frac{\eta_1}{2} \\ \sinh \frac{\eta_1}{2} & \cosh \frac{\eta_1}{2} \end{pmatrix}, \quad (2.31)$$

where

$$\begin{aligned} g_{BTZ} &= \begin{pmatrix} \frac{2}{M} \rho \exp(Mx) & \frac{2}{M} \sqrt{\rho^2 - M^2} \exp(M\tau) \\ \frac{2}{M} \sqrt{\rho^2 - M^2} \exp(-M\tau) & \frac{2}{M} \rho \exp(-Mx) \end{pmatrix}|_{x=0} \\ g_{AdS_3} &= \begin{pmatrix} R \cos t & R \sin t \\ -R \sin t & R \cos t \end{pmatrix}. \end{aligned} \quad (2.32)$$

The sigma model in (2.19) admits independent left and right $SL(2, R)$ symmetries. In (2.31), we have chosen to act by the same $SL(2, R)$ element both from the left and right. The left and right action on the group element g_{AdS_3} are the same. From this relation, it is easy to see that evaluating the charges we obtain

$$Q_L^{(1)}|_{BTZ} = 0, \quad Q_L^{(2)}|_{BTZ} = -\kappa \sinh \eta_1, \quad Q_L^{(3)}|_{BTZ} = \kappa \cosh \eta_1. \quad (2.33)$$

Proceeding similarly, we can evaluate the right $SL(2, R)$ charges, they are given by

$$\begin{aligned} Q_R^{(1)} &= -\frac{\dot{\rho}}{\sqrt{\rho^2 - M^2}} \cosh M(\tau + x) + \frac{(\dot{x} - \dot{\tau})}{M} \rho \sqrt{\rho^2 - M^2} \sinh M(\tau + x), \\ Q_R^{(2)} &= \frac{\rho^2 - M^2}{M} \dot{\tau} - \frac{\rho^2}{M} \dot{x}, \\ Q_R^{(3)} &= \frac{\dot{\rho}}{\sqrt{\rho^2 - M^2}} \sinh M(\tau + x) + \frac{(\dot{\tau} - \dot{x})}{M} \rho \sqrt{\rho^2 - M^2} \cosh M(\tau + x). \end{aligned} \quad (2.34)$$

Again, substituting the initial conditions (2.18) in these charges, we obtain

$$Q_R^{(1)}|_{BTZ} = 0, \quad Q_R^{(2)}|_{BTZ} = \kappa \sinh \eta_1, \quad Q_R^{(3)}|_{BTZ} = \kappa \cosh \eta_1. \quad (2.35)$$

This of course is related to charge in AdS_3 by a $SO(1, 2)$ boost

$$\begin{pmatrix} Q_R^{(1)} \\ Q_R^{(2)} \\ Q_R^{(3)} \end{pmatrix}_{BTZ} = \begin{pmatrix} 1 & 0 & 0 \\ 0 & \cosh \eta_1 & \sinh \eta_1 \\ 0 & \sin \eta_1 & \cosh \eta_1 \end{pmatrix} \begin{pmatrix} Q_R^{(1)} \\ Q_R^{(2)} \\ Q_R^{(3)} \end{pmatrix}_{AdS_3}. \quad (2.36)$$

We can verify the result for the charges in (2.35) by using the relationship between the group elements of the geodesics in AdS_3 and BTZ in (2.66).

It is useful to evaluate the quadratic Casimir of these charges, which are given by

$$Q_L \cdot Q_L = (Q_L^{(1)})^2 + (Q_L^{(2)})^2 - (Q_L^{(3)})^2 \quad (2.37)$$

Evaluating this for the time-like geodesic in AdS_3 , we obtain

$$Q_L \cdot Q_L|_{AdS_3} = -\kappa^2 \quad (2.38)$$

For the geodesic on BTZ, we obtain

$$\begin{aligned} Q_L \cdot Q_L|_{BTZ} &= \rho^2 \dot{x}^2 + \frac{\dot{\rho}^2}{\rho^2 - M^2} - (\rho^2 - M^2) \dot{\tau}^2, \\ &= -\kappa^2. \end{aligned} \quad (2.39)$$

To obtain the last line, we have substituted the initial conditions of the geodesic in (2.18). Similarly, the quadratic Casimir of the right charges is given by

$$Q_R \cdot Q_R = (Q_R^{(1)})^2 + (Q_R^{(2)})^2 - (Q_R^{(3)})^2. \quad (2.40)$$

Evaluating this on the AdS_3 geodesic results in

$$Q_R \cdot Q_R|_{AdS_3} = -\kappa^2. \quad (2.41)$$

For BTZ, we obtain

$$\begin{aligned} Q_R \cdot Q_R|_{BTZ} &= \rho^2 \dot{x}^2 + \frac{\dot{\rho}^2}{\rho^2 - M^2} - (\rho^2 - M^2) \dot{\tau}^2, \\ &= -\kappa^2. \end{aligned} \quad (2.42)$$

As the charges for the AdS_3 geodesic and BTZ are related by an $SO(1, 2)$ boost, the resulting Casimir is the same. This fact is useful to construct classical string solutions, as we will see subsequently.

2.2 In-falling particle with longitudinal velocity

We now generalise the co-ordinate transformation in (2.5), the following

$$\begin{aligned} X_0 &= \sqrt{r^2 + R^2} \sin t = \frac{R}{M} \left[\sqrt{\rho^2 - M^2} \sinh(M\tau) \cosh \eta_2 - \rho \sinh \eta_2 \sinh(Mx) \right], \\ X_1 &= \sqrt{r^2 + R^2} \cos t = \frac{R}{M} \left[\rho \cosh \eta_1 \cosh(Mx) - \sqrt{\rho^2 - M^2} \sinh \eta_1 \cosh(M\tau) \right], \\ X_2 &= r \sin \phi = \frac{R}{M} \left[\rho \sinh(Mx) \cosh \eta_2 - \sqrt{\rho^2 - M^2} \sinh(M\tau) \sinh \eta_2 \right], \\ X_3 &= r \cos \phi = \frac{R}{M} \left[\sqrt{\rho^2 - M^2} \cosh \eta_1 \cosh(M\tau) - \rho \sinh \eta_1 \cosh(Mx) \right]. \end{aligned} \quad (2.43)$$

In comparison with the earlier transformation, we now have a boost η_2 also in the X_0, X_2 plane, along with the boost η_1 in the X_1, X_3 plane. Let us study what happens to the time-like geodesic at the origin in the AdS_3 coordinates given by (2.6). In the BTZ coordinates, this trajectory satisfies the condition

$$\begin{aligned}\rho \sinh(Mx) \cosh \eta_2 &= \sqrt{\rho^2 - M^2} \sinh(M\tau) \sinh \eta_2, \\ \sqrt{\rho^2 - M^2} \cosh \eta_1 \cosh(M\tau) &= \rho \sinh \eta_1 \cosh(Mx).\end{aligned}\quad (2.44)$$

These relations arise from setting $r = 0$ in the last 2 equations of (2.43). Now using these relations in the first equation of (2.43), we obtain

$$\begin{aligned}R \sin t &= \frac{R}{M} \sqrt{\rho^2 - M^2} \frac{\sinh M\tau}{\cosh \eta_2}, \\ &= \frac{R}{M} \frac{\rho \sinh Mx}{\sinh \eta_2},\end{aligned}\quad (2.45)$$

From the the 2nd equation of (2.43), we obtain

$$\begin{aligned}R \cos t &= \frac{R}{M} \frac{\rho \cosh Mx}{\cosh \eta_1}, \\ &= \frac{R}{M} \sqrt{\rho^2 - M^2} \frac{\cosh M\tau}{\sinh \eta_1}.\end{aligned}\quad (2.46)$$

From these equations we see that

$$\begin{aligned}\rho^2 \left[\left(\frac{\sinh Mx}{\sinh \eta_2} \right)^2 + \left(\frac{\cosh Mx}{\cosh \eta_1} \right)^2 \right] &= M^2, \\ (\rho^2 - M^2) \left[\left(\frac{\sinh M\tau}{\cosh \eta_2} \right)^2 + \left(\frac{\cosh M\tau}{\sinh \eta_1} \right)^2 \right] &= M^2.\end{aligned}\quad (2.47)$$

Constants of motion along geodesics

The equations (2.44), (2.45), (2.46) describe the trajectory of an in-falling particle in BTZ but with velocity in the x direction. To see this, we differentiate the 2nd equation of (2.45) with respect to σ^0 and use (2.46) to obtain

$$\frac{1}{\sinh \eta_2} \left(\dot{\rho} \sinh Mx + \rho M \dot{x} \cosh Mx \right) = \kappa \rho \frac{\cosh Mx}{\cosh \eta_1}. \quad (2.48)$$

Similarly differentiating the first equation of (2.46) and using the second equation of (2.45) we get

$$\frac{1}{\cosh \eta_1} \left(\dot{\rho} \cosh Mx + \rho M \dot{x} \sinh Mx \right) = -\kappa \rho \frac{\sinh Mx}{\sinh \eta_2}. \quad (2.49)$$

Solving for \dot{x} from (2.48) and (2.49) and using (2.47), we obtain

$$\rho^2 \dot{x} = M \kappa \cosh \eta_1 \sinh \eta_2. \quad (2.50)$$

Comparing with (2.13), we see that this is clearly the equation for the constant of motion for the momentum along the x -direction for a geodesic in the BTZ geometry. Note that the velocity \dot{x} is non-zero only when the boost parameter η_2 does not vanish. Proceeding along similar lines, we can differentiate the first equation in (2.45) and the second equation in (2.46) to obtain

$$\begin{aligned} \frac{1}{\cosh \eta_2} \left(\frac{\rho \dot{\rho}}{\sqrt{\rho^2 - M^2}} \sinh M\tau + M \sqrt{\rho^2 - M^2} \dot{\tau} \cosh M\tau \right) &= \kappa \sqrt{\rho^2 - M^2} \frac{\cosh M\tau}{\sinh \eta_1}, \\ \frac{1}{\sinh \eta_1} \left(\frac{\rho \dot{\rho}}{\sqrt{\rho^2 - M^2}} \cosh M\tau + M \sqrt{\rho^2 - M^2} \dot{\tau} \sinh M\tau \right) &= -\kappa \sqrt{\rho^2 - M^2} \frac{\sinh M\tau}{\cosh \eta_2} \end{aligned} \quad (2.51)$$

Solving for $\dot{\tau}$ from these equations and using the second equation in (2.47), we obtain

$$(\rho^2 - M^2) \dot{\tau} = M \kappa \cosh \eta_2 \sinh \eta_1. \quad (2.52)$$

This is the constant of motion due to the time translation symmetry of the BTZ metric (2.13). Now taking the ratio of (2.50), (2.52) we obtain

$$\frac{\rho^2}{\rho^2 - M^2} \dot{x} = \tanh \eta_2 \coth \eta_1 \dot{\tau}. \quad (2.53)$$

Radial equation along the geodesic

We now need to find the geodesic equation for the radial coordinate. This involves several manipulations with the basic equations relating the trajectory in AdS_3 and BTZ. From the 2 equations in (2.44), we can solve for $\cosh Mx$,

$$(\cosh Mx)^2 = \frac{1}{\rho^2} \frac{(\rho^2 - M^2)(\tanh \eta_2)^2 - \rho^2}{(\tanh \eta_2 \tanh \eta_1)^2 - 1}. \quad (2.54)$$

Using this in the second equation of (2.44), we also have

$$(\cosh M\tau)^2 = \frac{(\tanh \eta_1)^2}{\rho^2 - M^2} \frac{(\rho^2 - M^2)(\tanh \eta_2)^2 - \rho^2}{(\tanh \eta_2 \tanh \eta_1)^2 - 1}. \quad (2.55)$$

Differentiating the second equation in (2.44) and eliminating the \dot{x} term using (2.53), we obtain

$$\sinh M\tau \left(1 - \frac{\rho^2 - M^2}{\rho^2} (\tanh \eta_1)^2 \right) \dot{\tau} = -\frac{M \dot{\rho}}{(\rho^2 - M^2)^{\frac{3}{2}}} \tanh \eta_1 \cosh Mx. \quad (2.56)$$

By squaring this equation and using (2.54), we can write

$$\begin{aligned} (\sinh M\tau)^2 \dot{\tau}^2 &= -\frac{M^2 \dot{\rho}^2}{(\rho^2 - M^2)} \\ &\times \frac{\rho^2}{\rho^2 - (\rho^2 - M^2) \tanh^2 \eta_2} \times \frac{\tanh^2 \eta_1}{\tanh^2 \eta_2 \tanh^2 \eta_1 - 1}. \end{aligned} \quad (2.57)$$

We can eliminate $\dot{\tau}$ using the conservation equation (2.52), to obtain

$$\begin{aligned} \kappa^2 \sinh^2 M\tau &= -\frac{\dot{\rho}^2}{\rho^2 - M^2} \\ &\times \frac{1}{\sinh^2 \eta_2 \sinh^2 \eta_1 - \cosh^2 \eta_2 \cosh^2 \eta_1} \times \frac{\rho^2}{\rho^2 - (\rho^2 - M^2) \tanh^2 M\eta_2}. \end{aligned} \quad (2.58)$$

Now using the (2.55) and (2.58), we can eliminate the τ dependence to obtain

$$\begin{aligned} -\frac{\kappa^2}{\rho^2} \left[\rho^2 - (\rho^2 - M^2)(\tanh \eta_2)^2 \right] \left[(\sinh \eta_2 \sinh \eta_1)^2 - (\cosh \eta_2 \cosh \eta_1)^2 \right] \\ = \frac{\kappa^2}{\rho^2(\rho^2 - M^2)} (\sinh \eta_1 \cosh \eta_2)^2 \left[(\rho^2 - M^2)(\tanh \eta_2)^2 - \rho^2 \right]^2 - \frac{\dot{\rho}^2}{\rho^2 - M^2}. \end{aligned} \quad (2.59)$$

Opening up the terms and re-grouping, we obtain

$$-\frac{\dot{\rho}^2}{\rho^2 - M^2} - \frac{(\kappa M \sinh \eta_2 \cosh \eta_1)^2}{\rho^2} + \frac{(\kappa M \sinh \eta_1 \cosh \eta_2)^2}{\rho^2 - M^2} = \kappa^2. \quad (2.60)$$

We see that this equation coincides the radial equation of the geodesic in BTZ given in (2.15). Using (2.50), (2.52) and (2.60), we can identify the constants of motion to be

$$\frac{E}{R^2} = -\kappa M \sinh \eta_1 \cosh \eta_2, \quad \frac{v}{R^2} = M \kappa \cosh \eta_1 \sinh \eta_2, \quad \frac{\tilde{m}^2}{R^2} = \kappa^2. \quad (2.61)$$

Left and right $SL(2, R)$ charges

We can also find the initial conditions at $\sigma^0 = 0$, when the geodesic has zero radial velocity $\dot{\rho}(0) = 0$.

$$\begin{aligned} x(0) = 0, \quad \dot{x}(0) = \frac{\kappa}{M} \frac{\sinh \eta_2}{\cosh \eta_1}, \quad \tau(0) = 0, \quad \dot{\tau}(0) = \frac{\kappa}{M} \frac{\cosh \eta_2}{\sinh \eta_1}. \\ \rho(0) = M \cosh \eta_1, \quad \dot{\rho}(0) = 0. \end{aligned} \quad (2.62)$$

These initial conditions are obtained by solving (2.60) and (2.47), together with the conservation equations (2.50), (2.52). With these initial conditions, we can find the left and right $SL(2, R)$ charges in (2.27), (2.34). For the left charges, we obtain

$$Q_L^{(1)}|_{BTZ} = 0, \quad Q_L^{(2)}|_{BTZ} = -\kappa \sinh(\eta_1 + \eta_2), \quad Q_R^{(1)}|_{BTZ} = \kappa \cosh(\eta_1 + \eta_2). \quad (2.63)$$

Similarly, evaluating the right charges, we get

$$Q_R^{(1)}|_{BTZ} = 0, \quad Q_R^{(2)}|_{BTZ} = \kappa \sinh(\eta_1 - \eta_2), \quad Q_R^{(1)}|_{BTZ} = \kappa \cosh(\eta_1 - \eta_2). \quad (2.64)$$

It is clear that the $Q_L|_{BTZ}, Q_R|_{BTZ}$ charges for the geodesic with velocity can be obtained from the charges of the time-like geodesic at the origin of AdS_3 by the boosts in (2.29), (2.36)

by replacing the boost parameter to $\eta_1 \rightarrow \eta_1 + \eta_2$ and $\eta_1 \rightarrow \eta_1 - \eta_2$ respectively. This fact can also be seen, from the transformation in (2.43), on the geodesic we have the relations

$$\begin{aligned} X_0 \cosh \eta_2 + X_2 \sinh \eta_2 &= R \sin t \cos \eta_2 = \frac{R}{M} \sqrt{\rho^2 - M^2} \sinh M\tau, \\ X_1 \cosh \eta_1 + X_3 \sinh \eta_1 &= R \cos t \cosh \eta_1 = \frac{R}{M} \rho \cosh Mx, \\ X_2 \cosh \eta_2 + X_0 \sinh \eta_2 &= R \sin t \sinh \eta_2 = \frac{R}{M} \rho \sinh Mx, \\ X_3 \cos \eta_1 + X_1 \sinh \eta_1 &= R \cos t \sinh \eta_1 = \frac{R}{M} \sqrt{\rho^2 - M^2} \cosh M\tau. \end{aligned} \quad (2.65)$$

On the geodesic, the $SL(2, R)$ element parameterised by BTZ co-ordinates is related to that of AdS_3 by

$$g_{BTZ} = \begin{pmatrix} \cosh \frac{\eta_1 + \eta_2}{2} & \sinh \frac{\eta_1 + \eta_2}{2} \\ \sinh \frac{\eta_1 + \eta_2}{2} & \cosh \frac{\eta_1 + \eta_2}{2} \end{pmatrix} g_{AdS_3} \begin{pmatrix} \cosh \frac{\eta_1 - \eta_2}{2} & \sinh \frac{\eta_1 - \eta_2}{2} \\ \sinh \frac{\eta_1 - \eta_2}{2} & \cosh \frac{\eta_1 - \eta_2}{2} \end{pmatrix}, \quad (2.66)$$

where

$$\begin{aligned} g_{BTZ} &= \begin{pmatrix} \frac{2}{M} \rho \exp(Mx) & \frac{2}{M} \sqrt{\rho^2 - M^2} \exp(M\tau) \\ \frac{2}{M} \sqrt{\rho^2 - M^2} \exp(-M\tau) & \frac{2}{M} \rho \exp(-Mx) \end{pmatrix}, \\ g_{AdS_3} &= \begin{pmatrix} R \cos t & R \sin t \\ -R \sin t & R \cos t \end{pmatrix}. \end{aligned} \quad (2.67)$$

This relation between the group elements also enables the easy evaluation of the charges, and we obtain the results (2.63), (2.64) for the left and right $SL(2, R)$ charges. Since the left and the right $SL(2, R)$ charges are related by a boost, the quadratic Casimir of these charges remains invariant, and the relations (2.39), (2.42) continue to hold.

3 In-falling classical strings in BTZ

In $AdS_3 \times S^3 \times M$ several classical string solutions are constructed as follows: One considers the time like a geodesic at the origin of AdS_3 , and a classical solution of the sigma model on S^3 such that the solution satisfies the classical Virasoro condition. To proceed further, we describe some aspects of the $SU(2)$ WZW model, it is given by the action

$$S_{SU(2)} = -\frac{k}{8\pi} \int_{\Sigma} d^2\sigma \operatorname{Tr} [\hat{g}^{-1} \partial_a \hat{g} \hat{g}^{-1} \partial^a \hat{g}] + \frac{k}{12\pi} q \int_{\mathcal{B}} \operatorname{Tr} [\hat{g}^{-1} d\hat{g} \wedge \hat{g}^{-1} d\hat{g} \wedge \hat{g}^{-1} d\hat{g}]. \quad (3.1)$$

Here $\hat{g} \in SU(2)$ which can be expressed as

$$g = \begin{pmatrix} Z_1 & Z_2 \\ -Z_2^* & Z_1^* \end{pmatrix}, \quad |Z_1|^2 + |Z_2|^2 = 1. \quad (3.2)$$

Again q lies between 0 and 1. It is 0 for the background with pure RR flux and 1 for the pure NS flux and $\alpha'k = R^2$ ¹. Classically, the model admits $SU(2)_L, SU(2)_R$ conserved charges which are given by

$$\hat{Q}_L = \frac{k}{2\pi} \int_0^{2\pi} d\sigma^1 \left(\hat{g}^{-1} \dot{\hat{g}} + q \hat{g}^{-1} \dot{\hat{g}}' \right), \quad \hat{Q}_R = \frac{k}{2\pi} \int_0^{2\pi} d\sigma^1 \left(\dot{\hat{g}} \hat{g}^{-1} - q \dot{\hat{g}}' \hat{g}^{-1} \right). \quad (3.3)$$

We can project these charges along the 3 generators of $SU(2)$ by defining

$$J_L^i = ik \operatorname{Tr}[\zeta^i \cdot \hat{Q}_L], \quad J_R^i = ik \operatorname{Tr}[\zeta^i \cdot \hat{Q}_R], \quad (3.4)$$

where

$$\zeta^1 = \frac{1}{2} \sigma^1, \quad \zeta^2 = \frac{1}{2} \sigma^2, \quad \zeta^3 = \frac{1}{2} \sigma^3. \quad (3.5)$$

To make matters more explicit, it is useful to have a parametrisation of the group element in $SU(2)$ by

$$Z_1 = X_1 + iX_2 = \sin \psi e^{i\phi_1}, \quad Z_2 = X_3 + iX_4 = \cos \psi e^{i\phi_2}. \quad (3.6)$$

The metric on the sphere, then, is given by

$$ds_{S^3}^2 = d\psi^2 + \sin^2 \psi d\phi_1^2 + \cos^2 \psi d\phi_2^2. \quad (3.7)$$

Let us choose the B_{NS} field to be given by²

$$B_{\phi_1 \phi_2} = q \sin^2 \psi = \frac{q}{2} (\cos 2\psi - 1). \quad (3.8)$$

We can add a constant to the field B , and it does not affect the equations of motion. Quite often, it is convenient to choose the following combination of angular momenta J_1 and J_2 which generate the shift in ϕ_1 and ϕ_2

$$J_1 = -\frac{1}{2} (J_R^3 + J_L^3), \quad J_2 = -\frac{1}{2} (J_R^3 - J_L^3). \quad (3.9)$$

Consider any classical solution in S^3 , say, geodesics on S^3 , circular strings and giant magnons moving on a time-like geodesic at the origin on AdS_3 and at a fixed point on M . These are solutions to the equation of motion of the sigma model; they are valid classical solutions of the string theory as long as the Virasoro constraints are satisfied.

$$\begin{aligned} T_{00}(AdS_3) + T_{00}(S^3) + T_{00}(M) &= 0, \\ T_{01}(AdS_3) + T_{01}(S^3) + T_{01}(M) &= 0. \end{aligned} \quad (3.10)$$

Here we have used $T_{00} = T_{11}, T_{01} = T_{10}$ to write down the non-trivial constraints. Geodesics, circular strings and giant magnons satisfy the constraint $T_{01}(S^3) = 0$, when evaluated on

¹In case $M = S^3 \times S^1$, then the levels of the 2 $SU(2)$ WZW models are related to the level of the $SL(2, R)$ WZW model. For eg. if $q = 1$, then $\frac{1}{k} = \frac{1}{k_1} + \frac{1}{k_2}$ where k_1, k_2 are the levels of the 2 $SU(2)$ models [16].

²An additive constant to the B_{NS} field shifts the sigma model action by a total derivative. We have chosen this constant c defined in [17] to be $c = -1$.

the respective classical solutions, as we will review subsequently. There is no contribution to the world sheet stress tensor from the sigma model on M since the string is at a fixed position on M , therefore we have $T_{01}(M) = 0$. Finally, since the solution is the time-like geodesic at the origin of AdS_3 with no dependence on the world sheet spatial direction, we have $T_{01}(AdS_3) = 0$. This implies the 2nd Virasoro constraint in (3.10) is satisfied. Now, the first Virasoro constraint on these solutions reduces to

$$-k\kappa^2 + T_{00}(S^3) = 0. \quad (3.11)$$

This discussion and the conclusions of section 2 then imply the following. Once we map the time-like geodesic to the in-falling geodesic in BTZ, it is guaranteed that the sigma model equations of motion in $BTZ \times S^3 \times M$ are satisfied. We can also see that the following Virasoro constraints are satisfied

$$\begin{aligned} T_{00}(BTZ) + T_{00}(S^3) + T_{00}(M) &= 0, \\ T_{01}(BTZ) + T_{01}(S^3) + T_{01}(M) &= 0. \end{aligned} \quad (3.12)$$

The 2nd Virasoro constraint in (3.12) is satisfied, since we still do not have world sheet spatial dependence in the BTZ and the world sheet momentum of each of these solutions vanish on S^3 and M . Finally, the first Virasoro constraint is satisfied due to the non-trivial observation in the previous section. The maps (2.5), (2.43), which take the time-like geodesic at the origin of AdS_3 to the in-falling geodesic in BTZ is such that the $SL(2, R)$ Casimir κ^2 is invariant as shown for example in (2.39), (2.42). The world sheet stress tensor in BTZ on solutions which depend only on world sheet time is given by

$$\begin{aligned} T_{00}(BTZ) &= k \left(-\frac{E^2}{R^4(\rho^2 - M^2)} + \frac{\dot{\rho}^2}{\rho^2 - M^2} + \frac{v^2}{R^4\rho^2} \right), \\ &= kQ_L \cdot Q_L = kQ_R \cdot Q_R, \\ &= -k\kappa^2. \end{aligned} \quad (3.13)$$

To obtain these results, we have used the identification of the quadratic Casimir with the world sheet stress tensor in BTZ from (2.39), (2.42). This then implies that the first Virasoro constraint (3.12) is satisfied if the solution satisfies the corresponding solution on AdS_3 . Therefore, we conclude that the map which takes the time like geodesic at the origin of AdS_3 also takes classical string solutions from $AdS_3 \times S^3 \times M$ to $BTZ \times S^3 \times M$. As we have emphasised, these classical string solutions involve geodesics in AdS_3 and BTZ. To make matters concrete, we will discuss the case of geodesics, circular strings and giant magnons on S^3 falling in BTZ.

Geodesics

Geodesics on S^3 falling into the BTZ horizon are given by

$$\begin{aligned} \rho(\sigma^0, \sigma^1) &= \rho(\sigma^0), & \tau(\sigma^0, \sigma^1) &= \tau(\sigma^0), & x(\sigma^0, \sigma^1) &= x(\sigma^0), \\ \psi(\sigma^0, \sigma^1) &= 0, & \phi_1(\sigma^0, \sigma^1) &= 0, & \phi_2(\sigma^0, \sigma^1) &= \frac{J}{k}\sigma^0, \\ X(\sigma^0, \sigma^1)|_M &= \text{constant}. \end{aligned} \quad (3.14)$$

where the BTZ co-ordinates $\{\rho, \tau, \sigma\}$ depend only on the world sheet time and are obtained by the maps (2.5), (2.43) and therefore, they satisfy the general geodesic equations (2.50), (2.52), (2.60). Let us evaluate the $SU(2)$ charges using (3.4).

$$J_{L,R}^1 = 0, \quad J_{L,R}^2 = 0, \quad J_L^3 = J, \quad J_R^3 = -J. \quad (3.15)$$

It is clear that the solution in (3.14) satisfies the 2nd Virasoro constraint (3.12). On evaluating the first Virasoro constraint, we obtain

$$-k\kappa^2 + \frac{1}{k}(J)^2 = 0, \quad T_{00}(S^3) = \frac{(J)^2}{k}. \quad (3.16)$$

We identify $\Delta = k\kappa$ and therefore, we obtain the BPS relation

$$\Delta = J. \quad (3.17)$$

It is important to realise that these solutions are geodesics falling into the horizon of the BTZ.

Circular Strings

The in-falling circular string in BTZ is given by

$$\begin{aligned} \rho(\sigma^0, \sigma^1) &= \rho(\sigma^0), & \tau(\sigma^0, \sigma^1) &= \tau(\sigma^0), & x(\sigma^0, \sigma^1) &= x(\sigma^0), \\ Z_1 &= \sqrt{\frac{W - qm}{2W}} e^{i[\sigma^0(W + qm) + m\sigma^1]}, & Z_2 &= \sqrt{\frac{W + qm}{2W}} e^{i[\sigma^0(W - qm) - m\sigma^1]}, \\ W &= \sqrt{w^2 + q^2m^2}, \\ X(\sigma^0, \sigma^1)|_M &= \text{constant}. \end{aligned} \quad (3.18)$$

Here $m \in \mathbb{Z}$, the trajectory in BTZ is that of a geodesic given by the equations (2.50), (2.52), (2.60), while the solution on the S^3 is the circular string solution found by [17] for the mixed Ramond-Ramond and NS flux, $q \neq 0$. The first Virasoro constraint in (3.10) is satisfied provided

$$\kappa^2 = \omega^2 + m^2. \quad (3.19)$$

We have again used equation (3.13) to evaluate the stress tensor of the solution in the BTZ direction. It can be seen that the second Virasoro is also satisfied. Evaluating the angular momenta of the solution on S^3 , we obtain

$$J_1 = J_2 = \frac{k}{2}(W - qm). \quad (3.20)$$

To complete the discussion, we write down the dispersion relations

$$\Delta = k\kappa = \sqrt{(J + qkm)^2 + k^2m^2(1 - q^2)}, \quad J \equiv J_1 + J_2 = 2J_1. \quad (3.21)$$

Expanding in the large J limit:

$$\Delta - J = qkm + \frac{k^2m^2(1 - q^2)}{2J} + \mathcal{O}(J^{-2}). \quad (3.22)$$

Again, we mention that the maps (2.5), (2.43), which take the time-like geodesic at the origin in AdS_3 to the in-falling geodesic in BTZ, ensure that the circular string solution in AdS_3 is a solution in BTZ with the same dispersion relation. We need to think of $\Delta = k\kappa$ as the quadratic Casimir in the $SL(2, R)$ WZW model.

Giant Magnon

For these classes of solutions, we consider the case of $q = 0$ and the simplest giant magnon solution. The discussion can be easily generalised for more general giant magnons found in [18] and for the solutions with $q \neq 0$ in [17] as we will outline subsequently. The simplest giant magnon solution in BTZ is obtained by the following string configuration

$$\begin{aligned} \rho(\sigma^0, \sigma^1) &= \rho(\sigma^0), & \tau(\sigma^0, \sigma^1) &= \tau(\sigma^0), & x(\sigma^0, \sigma^1) &= x(\sigma^0), \\ Z_1 &= \left[\sin \frac{p}{2} \tanh y - i \cos \frac{p}{2} \right] e^{i\tilde{\sigma}^0}, & Z_2 &= \frac{\sin \frac{p}{2}}{\cosh y}, \\ y &= \frac{\tilde{\sigma}^1 - \tilde{\sigma}^0 \cos \frac{p}{2}}{\sin \frac{p}{2}}, & \tilde{\sigma}^0 &= \kappa \sigma^0, & \tilde{\sigma}^1 &= \kappa \sigma^1. \end{aligned} \quad (3.23)$$

The S^3 part of the solution was found first in [19] and then discussed in detail in [18]. It can be verified that the solution satisfies the first Virasoro condition in (3.12), again, the reason this happens is because of the fact that the geodesic in BTZ satisfies the equation (3.13). Let us evaluate the charges

$$\begin{aligned} \Delta &= \frac{k}{2\pi} \int_{-\pi}^{\pi} d\sigma^1 \sqrt{-Q_L \cdot Q_L}, \\ &= k\kappa, \end{aligned} \quad (3.24)$$

where $Q_L \cdot Q_L$ is the $SL(2, R)$ Casimir defined in (2.37). The angular momenta of this solution are given by

$$J_1 = \frac{k}{2\pi} \int_{-\pi}^{\pi} d\sigma^1 \text{Im}[Z_1^* \partial_{\sigma^0} Z_1], \quad J_2 = \frac{k}{2\pi} \int_{-\pi}^{\pi} d\sigma^1 \text{Im}[Z_2^* \partial_{\sigma^0} Z_2]. \quad (3.25)$$

The giant magnon solution is obtained by taking the scaling limit

$$\kappa, \Delta, J_1 \rightarrow \infty \quad \text{with} \quad k, J_2, (\Delta - J_1), \sigma_0, \sigma_1 \quad \text{fixed.} \quad (3.26)$$

Evaluating the charges in this limit, we obtain

$$\begin{aligned} \Delta - J_1 &= \frac{k}{2\pi} \int_{-\infty}^{\infty} d\tilde{\sigma}^1 \left(1 - \text{Im}[Z_1^* \partial_{\tilde{\sigma}^1} Z_1] \right), \\ J_2 &= 0, \end{aligned} \quad (3.27)$$

where we have used (3.13).

$$\frac{\sqrt{-Q_L \cdot Q_L}}{\kappa} = 1. \quad (3.28)$$

Substituting the solution (3.23) in (3.27), we obtain

$$\Delta - J_1 = \frac{k}{\pi} \sin \frac{p}{2}. \quad (3.29)$$

We emphasise that the dispersion relation is again identical to that of the magnon in $AdS_3 \times S^3$, with Δ being identified as the quadratic Casimir in the $SL(2, R)$ WZW model.

For completeness, we mention that the boundary conditions the solution in (3.23) satisfies in the limit (3.26) is given by

$$\lim_{\tilde{\sigma}_1 \rightarrow \pm\infty} Z_1 = e^{i(\tilde{\sigma}_0 - \frac{\pi}{2} \pm \frac{p}{2})}, \quad \lim_{\tilde{\sigma}_1 \rightarrow \pm\infty} Z_2 = 0. \quad (3.30)$$

Therefore, the ends of the strings are at $\psi = \frac{\pi}{2}$ but at angles such that $\delta\phi_1 = p$. Considering several giant magnons, whose momentum is such that their sum vanishes, the second Virasoro condition in (3.12) can be satisfied. This is the same way the Virasoro condition for the case of magnons on $AdS_3 \times S^3$ is satisfied. It is clear that the embedding of the magnon in BTZ given in (3.23) can be extended for the general dyonic magnon solutions with charge $J_2 \neq 0$ found in [18] which obey the dispersion relation

$$\Delta - J_1 = \sqrt{J_2^2 + \frac{k^2}{\pi^2} \sin^2 \frac{p}{2}}. \quad (3.31)$$

We can also generalise the embedding for the giant magnons solutions in the presence of NS flux $q \neq 0$, found in [17]. All we have to do is take the BTZ part of the solution to be the in-falling geodesic obeying the trajectory (2.50), (2.52), (2.60) and the S^3 part to be that constructed in the earlier works.

4 Plane wave spectra in BTZ

In section 3, we demonstrated that the classical solutions of the string sigma model $AdS_3 \times S^3 \times M$ can be mapped to solutions in $BTZ \times S^3 \times M$. These solutions involve the time-like geodesics at the origin of AdS_3 , which are mapped to an in-falling geodesic in BTZ. We also showed that the solutions obey an identical dispersion relation once the conformal dimension Δ^2 is identified with the quadratic Casimir of the WZW model on BTZ. The plane wave limit of $AdS_3 \times S^3 \times M$ [12], involves a time-like geodesic at the origin with angular momentum along one of the circles of S^3 . The observations in section 3 suggest that it should be possible to obtain the same plane wave geometry in $BTZ \times S^3 \times M$ by zooming in the geometry around in-falling geodesics in BTZ. Contrary to the above argument, it is known that Penrose limit around generic geodesics in black hole backgrounds leads to time-dependent singular plane waves [20, 21]. Let us briefly review these results to place the observation for the Penrose limit for in-falling geodesics in the BTZ black hole in a relevant context. Consider the Schwarzschild black hole in $AdS_5 \times S^5$, the metric is given in

$$ds^2 = -\left(r^2 + 1 - \frac{r_0^2}{r^2}\right)dt^2 + \frac{dr^2}{r^2 + 1 - \frac{r_0^2}{r^2}} + r^2(d\phi^2 + \sin^2 \phi d\Omega_3^2) + d\psi^2 + \sin^2 \psi d\Omega_4^3. \quad (4.1)$$

Consider the case of a null geodesic carrying angular momentum along ϕ , one of the circles in the AdS_5 directions. The trajectory of this geodesic is governed by the following equations

$$\begin{aligned} \left(r^2 + 1 - \frac{r_0^2}{r^2}\right)\dot{t} &= E, & r^2\dot{\phi} &= J, \\ \dot{r}^2 + \frac{J^2}{r^2} \left(r^2 + 1 - \frac{r_0^2}{r^2}\right) &= E^2, & \psi &= \frac{\pi}{2}. \end{aligned} \quad (4.2)$$

The procedure for taking the Penrose limit along this geodesic has been detailed in Appendix A. This results in the following pp wave metric in Brinkmann coordinates

$$ds^2 = 2dx^+dx^- + \left[Ax_1^2 + B(x_2^2 + x_3^2) \right] (dx^+)^2 + \sum_{i=1}^3 dx_i^2 + \sum_{a=1}^5 dy_a^2, \quad (4.3)$$

$$A = \frac{4J^2r_0^2}{r^6(x^+)}, \quad B = -\frac{2J^2r_0^2}{r^6(x^+)}.$$

In the coefficients A, B , we need to substitute for the radial coordinate r in terms of the affine parameter x^+ by solving the second equation in (4.2). The coordinates y_a originate from the sphere S^5 . Note that for a radially in-falling geodesic $J = 0$, the plane wave geometry (4.3) reduces to flat space. Thus, the geometry in general depends on time x^+ and has been shown to be singular at x^+ such that $r(x^+) = 0$ [20, 21]. Let us examine the situation in which the null geodesic has angular momentum along one of the angles of S^5 . The trajectory of this geodesic is determined by the equations

$$\left(r^2 + 1 - \frac{r_0^2}{r^2} \right) \dot{t} = E, \quad \dot{\psi} = J, \quad (4.4)$$

$$\dot{r}^2 + J^2 \left(r^2 + 1 - \frac{r_0^2}{r^2} \right) = E^2, \quad \dot{\phi} = \frac{\pi}{2}.$$

Zooming near this geodesic, the geometry reduces to the following plane wave metric

$$ds^2 = 2dx^+dx^- - J^2 \left[\left(1 - \frac{3r_0^4}{r^4} \right) x_1^2 + \left(1 + \frac{r_0^4}{r^4} \right) \vec{z}_3^2 + \vec{z}_4^2 \right] (dx^+)^2 + dx_1^2 + d\vec{z}_3^2 + d\vec{z}_4^2, \quad (4.5)$$

where \vec{z}_3 refers to the 3 co-ordinates that label \mathbb{R}^3 and \vec{z}_4 refers to the 4 co-ordinates that label \mathbb{R}^4 . The details of obtaining the Penrose limit, together with the value of the 5 form fluxes, are given in appendix A. Here again, the radial coordinate is a function of light cone time x^+ , which is determined by solving the radial equation in (4.4). This implies the metric (4.5) is time dependent and singular when $r(x^+) = 0$. On similar lines, considering a generic null geodesic purely in the BTZ geometry and taking the appropriate plane wave limit, we obtain flat space. This is because BTZ is locally AdS_3 and plane wave limits of geodesics in maximally symmetric spaces always lead to flat space [22]. It is possible that these facts about Penrose limits in the geometry of black holes in AdS , that Penrose limits in $BTZ \times S^3 \times M$ were not studied earlier. In this section, we show that the geometry of the Penrose limit of an in-falling geodesic in $BTZ \times S^3 \times M$ with angular momenta along S^3 is identical to the plane wave geometry obtained by examining the Penrose limit of a time-like geodesic in $AdS_3 \times S^3 \times M$. Therefore, the plane wave spectra for the world sheet theories in these geometries are identical

4.1 The Penrose limit of $BTZ \times S^3 \times S^3 \times S^1$

In this section, we obtain the plane wave limit $BTZ \times S^3 \times S^3 \times S^1$ on in-falling geodesics. We choose to study the case of $M = S^3 \times S^1$ with mixed Ramond-Ramond and NS fluxes

with angular momentum on both S^3 's. Studying this general case enables the possibility of taking limits so that we can obtain a situation with either pure Ramond-Ramond flux or only pure NS flux, and with angular momentum only on one of the S^3 . We will compare our result for the plane wave geometry with the plane wave limit of $AdS_3 \times S^3 \times S^3 \times S^1$ with mixed fluxes obtained in [23]. The gravity background of $BTZ \times S^3 \times S^3 \times S^2$ is given by

$$ds^2 = G_{\mu\nu} dx^\mu dx^\nu = R^2 ds_{BTZ}^2 + R_1^2 ds_{S_1^3}^2 + R_2^2 ds_{S_2^3}^2 + ds_{S^1}^2, \quad (4.6)$$

where

$$\begin{aligned} ds_{BTZ}^2 &= -(\rho^2 - M^2) d\tau^2 + \frac{d\rho^2}{(\rho^2 - M^2)} + \rho^2 dx^2, \\ ds_{S^3}^2 &= d\psi_1^2 + \sin^2 \psi_1 d\Omega_2^2, \quad ds_{\tilde{S}^3}^2 = d\psi_2^2 + \sin^2 \psi_2 d\tilde{\Omega}_2^2, \quad ds_{S^1}^2 = d\tilde{\Omega}_1^2. \end{aligned} \quad (4.7)$$

$d\Omega_2^2, d\tilde{\Omega}_2^2$ are metrics on unit 2-spheres and Ω_1 is the angle on the circle S^1 . Here, the radii R , R_1 , and R_2 must satisfy the following condition to ensure the background solves the consistency condition of string theory in 10 dimensions. This leads to the constraint [16].

$$\frac{R^2}{R_1^2} + \frac{R^2}{R_2^2} = 1. \quad (4.8)$$

Following [23], we parametrise this relation as

$$\frac{R^2}{R_1^2} = \alpha \equiv \cos^2 \varphi, \quad \frac{R^2}{R_2^2} = 1 - \alpha \equiv \sin^2 \varphi. \quad (4.9)$$

The solution is supported by both NS fluxes and Ramond-Ramond fluxes, which are given by

$$\begin{aligned} H &= dB_{NS} = 2qR^2 \left[\text{Vol}(BTZ) + \frac{1}{\cos^2 \varphi} \text{Vol}(S^3) + \frac{1}{\sin^2 \varphi} (\tilde{S}^3) \right], \\ F &= 2\sqrt{1 - q^2}R^2 \left[\text{Vol}(BTZ) + \frac{1}{\cos^2 \varphi} \text{Vol}(S^3) + \frac{1}{\sin^2 \varphi} (\tilde{S}^3) \right], \end{aligned} \quad (4.10)$$

where

$$\begin{aligned} \text{Vol}(BTZ) &= \rho d\tau \wedge \rho \wedge dx, & \text{Vol}(S^3) &= \sin^2 \psi_1 d\psi_1 \wedge \text{Vol}S^2, \\ \text{Vol}(\tilde{S}^3) &= \sin^2 \psi_2 d\psi_2 \wedge \text{Vol}\tilde{S}^2. \end{aligned} \quad (4.11)$$

In (4.10), $0 \leq q \leq 1$ is the parameter which dials between a background supported by pure NS flux and that supported by pure Ramond-Ramond flux. Consider now an in-falling geodesic in this background whose trajectory obeys the equations ³

$$\begin{aligned} \dot{\tau} &= \frac{E}{(\rho^2 - \rho_+^2)}, & \dot{x} &= \frac{v}{\rho^2}, \\ \dot{\psi}_1 &= \frac{\alpha'}{R^2} \cos^2 \varphi J_1, & \dot{\psi}_2 &= \frac{\alpha'}{R^2} \sin^2 \varphi J_2. \end{aligned} \quad (4.12)$$

³To relate factors: α' in this paper is equal to $2\pi\alpha'$ in [23].

The reason for the normalisations in the angular velocity is that the angular momentum from the Noether definition is defined as J_1 . This can be seen as follows, from the Noether definition of the charge corresponding to shifts in ψ_1 , WZW model on S^2 at level k_1 , the angular momentum is given by

$$\begin{aligned} J_1 &= \frac{k_1}{2\pi} \int_0^{2\pi} \dot{\psi}_1 = \frac{R_1^2}{2\pi\alpha'} \int_0^{2\pi} \dot{\psi}_1, \\ &= \frac{R^2}{2\pi\alpha' \cos^2 \varphi} \int_0^{2\pi} \dot{\psi}_1. \end{aligned} \quad (4.13)$$

A very similar analysis explains the normalisation of the angular velocity $\dot{\psi}_2$ in (4.12). In the 2-spheres S^2, \tilde{S}^2 and the circle S^1 , let us choose the geodesic to be at a fixed angle $\frac{\pi}{2}$ in all directions. Since the geodesic is null in the $BTZ \times S^3 \times S^3 \times S^1$ background, we have the relation

$$\begin{aligned} \dot{\rho}^2 + \frac{\alpha'^2}{R^4} J^2 (\rho^2 - M^2) + v^2 \rho^{-2} (\rho^2 - M^2) &= E^2, \\ J^2 &= (J_1 \cos \varphi)^2 + (J_2 \sin \varphi)^2. \end{aligned} \quad (4.14)$$

Note that comparing the equations for $\dot{\tau}, \dot{x}, \dot{\rho}$ in (4.12), (4.14) with that in (2.50), (2.52) and (2.60), we see that the trajectory is that of the in-falling geodesic in BTZ. We can make the identifications

$$\begin{aligned} \kappa &= \frac{\alpha' J}{R^2} = \frac{J}{k} = \frac{\Delta}{k}, \\ \kappa M \sinh \eta_1 \cosh \eta_2 &= E, \quad \kappa M \sinh \eta_2 \cosh \eta_1 = v. \end{aligned} \quad (4.15)$$

In the first line in (4.15), we have used the definition $k\kappa = \Delta$. Furthermore, the constraint in the second line of (4.14) allows the introduction of 2 angles defined as

$$\cos \omega = \frac{J_1}{J} \cos \varphi, \quad \sin \omega = \frac{J_2}{J} \sin \varphi. \quad (4.16)$$

We perform the usual steps to take the Penrose limit along this geodesic. We first make the change of coordinates from $(\tau, \rho, x, \psi_1, \psi_2) \rightarrow (\lambda, \xi, \theta_0, \theta_1, \theta_2)$ which is given by

$$\begin{aligned} \tau &= \int_0^\lambda \dot{\tau} d\lambda' - \frac{\xi}{E} + v \theta_0 + \frac{J_1 \cos \varphi}{k} \theta_1 + \frac{J_2 \sin \varphi}{k} \theta_2, \\ \rho &= \int_0^\lambda \dot{\rho} d\lambda', \quad x = \int_0^\lambda \dot{x} d\lambda' + E \theta_0, \\ \psi_1 &= \cos \varphi \left[\cos \varphi \frac{J_1}{k} \lambda + E \theta_1 \right], \quad \psi_2 = \sin \varphi \left[\sin \varphi \frac{J_2}{k} \lambda + E \theta_2 \right], \\ \text{where } k &= \frac{R^2}{\alpha'}. \end{aligned} \quad (4.17)$$

We substitute this transformation in the metric (4.6), perform the following scaling

$$\begin{aligned} \lambda &\rightarrow \lambda, \quad \xi \rightarrow \frac{\xi}{R^2}, \quad \theta_i \rightarrow \frac{\theta_i}{R}, \quad i = 0, 1, 2 \\ \chi_a &\rightarrow \frac{\pi}{2} + \frac{\chi_a}{R_1}, \quad a \in \Omega_2, \quad \chi_a \rightarrow \frac{\pi}{2} + \frac{\chi_a}{R_2}, \quad a \in \tilde{\Omega}_2, \\ \Omega^1 &\rightarrow \frac{\Omega^1}{R}. \end{aligned} \quad (4.18)$$

Here χ_i refers to the angles of the 2-spheres $\Omega_1, \tilde{\Omega}_2$. We then take the following limit

$$R \rightarrow \infty, \quad \text{with} \quad \frac{R}{R_1}, \frac{R}{R_2} \quad \text{fixed.} \quad (4.19)$$

Substituting the transformation (4.17) in the metric (4.6) and expanding in the large R, R_1, R_2 limit we obtain

$$\begin{aligned} ds^2 = & 2d\lambda d\xi + \rho^2 [E^2 - \rho^{-2}v^2 f] d\theta_0^2 + \left[E^2 - \frac{\cos^2 \varphi}{k^2} f J_1^2 \right] d\theta_1^2 + \left[E^2 - \frac{\sin^2 \varphi}{k^2} f J_2^2 \right] d\theta_2^2 \\ & - 2f \left[\left(\frac{\cos \varphi}{k} v J_1 \right) d\theta_0 d\theta_1 + \left(\frac{\sin \varphi}{k} v J_2 \right) d\theta_0 d\theta_2 + \left(\frac{\sin \varphi \cos \varphi}{k^2} J_1 J_2 \right) d\theta_1 d\theta_2 \right] \\ & + \sin^2 \left(\frac{\cos^2 \varphi}{k} J_1 \lambda \right) ds^2(\mathbb{R}^2) + \sin^2 \left(\frac{\sin^2 \varphi}{k} J_2 \lambda \right) ds^2(\tilde{\mathbb{R}}^2) + ds^2(\mathbb{R}^1). \end{aligned} \quad (4.20)$$

Here $ds^2(\mathbb{R}^2)$ and similar expressions refers to the Euclidean metric on \mathbb{R}^2 and

$$f = \rho^2 - M^2. \quad (4.21)$$

This is the metric of the plane wave in Rosen coordinates. The transformation to the Brinkmann coordinates is easier once we diagonalise the metric in the directions θ_i . We first decouple θ_1, θ_2 by the following orthogonal transformation

$$\begin{aligned} \tilde{\theta}_1 &= \frac{J_1 \cos \varphi}{J} \theta_1 + \frac{J_2 \sin \varphi}{J} \theta_2, \\ \tilde{\theta}_2 &= -\frac{J_1 \sin \varphi}{J} \theta_1 + \frac{J_2 \cos \varphi}{J} \theta_2. \end{aligned} \quad (4.22)$$

This brings the metric (4.20) to the form

$$\begin{aligned} ds^2 = & 2d\lambda d\xi + \rho^2 [E^2 - \rho^{-2}v^2 f] d\theta_0^2 + \left[E^2 - \frac{J^2}{k^2} f \right] d\tilde{\theta}_1^2 - 2v f \frac{J}{k} d\theta_0 d\tilde{\theta}_1 + E^2 d\tilde{\theta}_2^2 \\ & + \sin^2 \left(\frac{\cos^2 \varphi}{k} J_1 \lambda \right) ds^2(\mathbb{R}^2) + \sin^2 \left(\frac{\sin^2 \varphi}{k} J_2 \lambda \right) ds^2(\tilde{\mathbb{R}}^2) + ds^2(\mathbb{R}^1). \end{aligned} \quad (4.23)$$

We now have to decouple θ_0 and $\tilde{\theta}_1$; let us write the metric in this subspace explicitly.

$$\begin{aligned} d\tilde{s}^2 &= (d\theta_0, d\tilde{\theta}_1) A(\rho) \begin{pmatrix} d\theta_0 \\ d\tilde{\theta}_1 \end{pmatrix}, \\ A(\rho) &= \rho^2 \begin{pmatrix} E^2 - v^2 & -vj \\ -vj & -j^2 \end{pmatrix} + \begin{pmatrix} v^2 M^2 & vj M^2 \\ vj M^2 & E^2 + j^2 M^2 \end{pmatrix}, \quad j \equiv \frac{J}{k}. \\ &\equiv \rho^2 B + C \end{aligned} \quad (4.24)$$

To bring the matrix A to the diagonal form, we first perform an orthogonal transformation from the coordinates $(\theta_0, \tilde{\theta}_1) \rightarrow (\hat{\theta}_0, \hat{\theta}_1)$ to which C is diagonal. This transformation is independent of ρ and brings C to the following form

$$\begin{aligned} O^T C O &= \begin{pmatrix} c_- & 0 \\ 0 & c_+ \end{pmatrix}, \\ c_{\pm} &= \frac{1}{2} \left(E^2 + M^2(j^2 + v^2) \pm \sqrt{[E^2 + M^2(j^2 + v^2)]^2 - 4v^2 E^2 M^2} \right). \end{aligned} \quad (4.25)$$

When $v \neq 0$, none of the eigenvalues are zero. In this basis, we perform the re-scaling

$$(\hat{\theta}_0, \hat{\theta}_1) \rightarrow \left(\frac{\check{\theta}_0}{\sqrt{c_-}}, \frac{\check{\theta}_1}{\sqrt{c_+}} \right). \quad (4.26)$$

In the coordinates $(\check{\theta}_0, \check{\theta}_1)$, the matrix $C \rightarrow I$ has become the identity, and B has become \check{B} , a symmetric matrix. We now perform the final orthogonal transformation to make the matrix \check{B} a diagonal matrix. Note that this transformation will retain C as identity. This sequence of coordinate transformations, which are independent of ρ , has the following effect on the matrix $A(\rho)$

$$A(\rho) = B\rho^2 + C \rightarrow \begin{pmatrix} 1 + \lambda_+\rho^2 & 0 \\ 0 & 1 + \lambda_-\rho^2 \end{pmatrix}, \quad (4.27)$$

where $\lambda_{\pm} = \frac{E^2 + j^2 M^2 - v^2 \pm \sqrt{(E^2 + j^2 M^2)^2 - 2(E - jM)(E + jM)v^2 + v^4}}{2M^2 v^2}.$

Therefore from the metric in (4.23), we have arrived at the following metric

$$ds^2 = 2d\lambda d\xi + (1 + \lambda_+\rho^2) d\theta^2 + (1 + \lambda_-\rho^2) d\tilde{\theta}^2 + \sin^2 \left(\frac{\cos^2 \varphi}{k} J_1 \lambda \right) ds^2(\mathbb{R}^2) + \sin^2 \left(\frac{\sin^2 \varphi}{k} J_2 \lambda \right) ds^2(\tilde{\mathbb{R}}^2) + E^2 d\tilde{\theta}_2^2 + ds^2(\mathbb{R}^1). \quad (4.28)$$

Here we have labelled the final decoupled co-ordinates as $(\theta, \tilde{\theta})$. The plane wave metric in (4.23) is in the Rosen form, and since it is diagonal, we can go over to the Brinkmann co-ordinates. Let us recall the general procedure. Consider a metric of the form

$$ds^2 = 2d\lambda d\xi + \sum_{i=1}^8 C_i^2 (dy^i)^2. \quad (4.29)$$

We go to Brinkmann coordinates by the following coordinate transformation

$$\lambda = x^+, \quad \xi = x^- + \frac{1}{2} \sum_i \frac{1}{C_i} \left(\frac{\partial C_i}{\partial x^+} \right) x^i x^i, \quad y^i = C_i^{-1} x^i. \quad (4.30)$$

Then the metric becomes

$$\begin{aligned} ds^2 &= 2dx^+ dx^- + \left[\sum_i \frac{C''(x^+)}{C_i} x^i x^i \right] (dx^+)^2 + \sum_i dx^i dx^i \\ &= 2dx^+ dx^- + \sum_i (M_{ii} x^i x^i) (dx^+)^2 + \sum_i dx^i dx^i. \end{aligned}$$

To evaluate the matrix M , we first write the derivative with respect to λ in terms of the derivative with respect to ρ as,

$$\frac{d^2}{d\lambda^2} = \frac{d}{d\lambda} \left(\dot{\rho} \frac{d}{d\rho} \right) = \dot{\rho}^2 \frac{d^2}{dr^2} + \dot{\rho} \left(\frac{d\dot{\rho}}{d\rho} \right) \frac{d}{d\rho}. \quad (4.31)$$

Carrying out this procedure on the metric in (4.28), we obtain

$$ds^2 = 2dx^+dx^- - \left[j^2(x_1^2 + x_2^2) + \frac{\cos^4 \varphi}{k^2} J_1^2(x_3^2 + x_4^2) + \frac{\sin^4 \varphi}{k^2} J_2^2(x_5^2 + x_6^2) \right] (dx^+)^2 + \sum_{i=1}^8 dx^i dx^i. \quad (4.32)$$

This is a homogeneous plane wave metric with masses in 6 directions. It is important to note that the masses in the directions x_1, x_2 result because of the precise form of the metric in $\theta, \tilde{\theta}$ directions in (4.28) and the values of λ_{\pm} in (4.27). We can express J_1, J_2 in terms of the angles introduced in (4.16), this results in

$$ds^2 = 2dx^+dx^- - j^2 [(x_1^2 + x_2^2) + \cos^2 \varphi \cos^2 \omega (x_3^2 + x_4^2) + \sin^2 \varphi \sin^2 \omega (x_5^2 + x_6^2)] (dx^+)^2 + \sum_{i=1}^8 dx^i dx^i. \quad (4.33)$$

We can now compare this metric to that obtained by taking the plane wave limit of the time-like geodesic at the origin in $AdS_3 \times S^3 \times S^3 \times S^1$ with angular momentum along S^1 's in the 3-spheres obtained in [23]⁴. We see that the mass matrix precisely agrees. Let us now examine the limiting forms of the background fluxes. We take limits of each component of the fluxes in (4.10), by performing the coordinate transformation in (4.17) and then performing the scaling (4.18) and taking the limit (4.19).

$$\begin{aligned} R^2 \text{Vol}(BTZ) &= R^2 \rho d\tau \wedge d\rho \wedge dx \\ &= R^2 \rho \left(\dot{\tau} d\lambda - \frac{d\xi}{E} + v d\theta_0 + \frac{J_1 \cos^2 \varphi}{k} d\theta_1 + \frac{J_2 \sin^2 \varphi}{k} d\theta_2 \right) \wedge \dot{\rho} d\lambda \wedge (\dot{x} d\lambda + E d\theta_0). \end{aligned} \quad (4.34)$$

Now performing the scaling (4.18), taking the large R limit and using the transformation (4.22), we obtain

$$\begin{aligned} \lim_{R \rightarrow \infty} R^2 \text{Vol}(BTZ) &= \rho \dot{\rho} E \left(\frac{J_1 \cos^2 \varphi}{k} d\theta_1 + \frac{J_2 \sin^2 \varphi}{k} d\theta_2 \right) \wedge d\lambda \wedge d\theta_0 \\ &= j E \rho \dot{\rho} d\tilde{\theta}_1 \wedge d\lambda \wedge d\theta_0. \end{aligned} \quad (4.35)$$

To proceed further, observe that,

$$E \rho \dot{\rho} = \left(\det A(\rho) \right)^{\frac{1}{2}} = v E M \sqrt{(1 + \lambda_+ \rho^2)(1 + \lambda_- \rho^2)}. \quad (4.36)$$

This, together with the fact scaling of the co-ordinates in (4.26), implies that we can write

$$\begin{aligned} \lim_{R \rightarrow \infty} R^2 \text{Vol}(BTZ) &= j d\lambda \wedge \left(\sqrt{1 + \lambda_+ \rho^2} d\theta \right) \wedge \left(\sqrt{1 + \lambda_- \rho^2} d\tilde{\theta} \right) \\ &= j dx^+ \wedge dx_1 \wedge dx_2. \end{aligned} \quad (4.37)$$

⁴Please see equation (2.20), (2.21), (2.22) of [23]. Note that the overall j in (4.33) can be scaled away by redefining x^+, x^- .

In the last line, we have used the transformation to the Brinkmann coordinates (4.30). Now, let us examine the fluxes on S^3

$$\begin{aligned} \frac{R^2}{\cos^2 \varphi} \text{Vol}(S^3) &= \frac{R^2}{\cos^2 \varphi} \sin^2 \psi_1 \, d\phi \wedge d\text{Vol}(S^2) \\ &= \frac{R^2}{\cos^2 \varphi} \sin^2 \left(\frac{\cos^2 \varphi}{k} J_1 \lambda + E \cos \varphi \theta_1 \right) \left(\frac{\cos^2 \varphi}{k} J_1 d\lambda + \cos \varphi E \, d\theta_1 \right) \wedge d\text{Vol}(S^2). \end{aligned} \quad (4.38)$$

We scale the co-ordinates as in (4.18) and take the $R \rightarrow \infty$ limit.

$$\begin{aligned} \lim_{R \rightarrow \infty} \frac{R^2}{\cos^2 \varphi} \text{Vol}(S^3) &= \frac{\cos^2 \varphi}{k} J_1 \sin^2 \left(\frac{\cos^2 \varphi}{k} J_1 \lambda \right) d\lambda \wedge d\text{Vol}(\mathbb{R}^2) \\ &= j \cos \varphi \cos dx^+ \wedge dx_3 \wedge dx_4. \end{aligned} \quad (4.39)$$

In the last line, we have used the definition (4.16) to relate J_1 to $\cos \omega$. Proceeding along similar lines, we obtain the limit

$$\lim_{R \rightarrow \infty} \frac{R^2}{\sin^2 \varphi} \text{Vol}(S_1^3) = j \sin \varphi \sin \omega dx^+ \wedge dx_5 \wedge dx_6. \quad (4.40)$$

From the limit in (4.37), (4.39) and (4.40), we see that in the plane wave limit, the fluxes are given by

$$\begin{aligned} H &= 2q \, dx^+ \wedge \left[J \, dx_1 \wedge dx_2 + \frac{\cos^2 \varphi}{\Delta} J_1 \, dx_3 \wedge dx_4 + \frac{\sin^2 \varphi}{\Delta} J_2 \, dx_5 \wedge dx_6 \right], \\ F &= 2\sqrt{1 - q^2} \, dx^+ \wedge \left[J \, dx_1 \wedge dx_2 + \frac{\cos^2 \varphi}{\Delta} J_1 \, dx_3 \wedge dx_4 + \frac{\sin^2 \varphi}{\Delta} J_2 \, dx_5 \wedge dx_6 \right]. \end{aligned} \quad (4.41)$$

The analysis of the Penrose limit can be repeated for the case $v = 0$ for which the metric $A(\rho)$ in (4.24) is diagonal⁵. It can be shown that we obtain the identical limit for the metric and fluxes. We see that the metric (4.33) and the fluxes (4.41) in the plane wave limit along the in-falling geodesic on $BTZ \times S^3 \times S^3 \times S^1$ and the Penrose limit along the time-like geodesic at the origin in $AdS_3 \times S^3 \times S^1$ obtained in [23] precisely agree. This implies that the spectrum of excitations of string theory in this plane wave background is identical to that in $AdS_3 \times S^3 \times S^1$. We will not repeat the analysis since it is identical to that done in [23]. In the case of the plane waves in BTZ , the light cone Hamiltonian is the charge

$$\begin{aligned} \mathcal{H} &= \Delta - \cos \varphi \cos \omega J_1 - \sin \varphi \sin \omega J_2, \\ &= k\sqrt{-Q_L \cdot Q_L} - \cos \varphi \cos \omega J_1 - \sin \varphi \sin \omega J_2. \end{aligned} \quad (4.42)$$

The second line arises because of the identification of the charge $\Delta = k\kappa$ along time-like geodesics in AdS_3 with the Casimir of the $SL(2, R)$ sigma model in the BTZ geometry, as shown for example in (2.39). It should be emphasised that the resultant geometry after the Penrose limit is independent of the initial conditions of the in-falling geodesic

⁵The analysis is simpler for $v = 0$ and it does not involve the diagonalization in (4.25).

and therefore true for any geodesic in-falling into the horizon of the BTZ geometry. The plane wave limit of the spectrum of the WZW model on $AdS_3 \times S^3 \times S^3 \times S^1$ also yields the same dispersion relation obtained by quantising the string theory on the plane wave geometry [23]. Since we have demonstrated that the geometry obtained in the region of the in-falling geodesic on $BTZ \times S^3 \times S^3 \times S^1$ is identical to that of the plane wave limit in the AdS_3 , it must be the case that there exists a limit of the spectrum of the WZW model on $BTZ \times S^3 \times S^3 \times S^1$ which results in identical spectrum as in case of AdS_3 . The approach would involve expanding the highest weight state in a direction which is boosted by the parameters η_1, η_2 . This is because we showed in section 2.2 that the charges of the time-like geodesics in AdS_3 , which are semi-classical states in the WZW model, are related to those of the in-falling geodesic in BTZ by an $SL(2, R)$ boost. These charges are time-like in the $SL(2, R)$ norm, as can be seen in (2.39) and (2.42). Therefore, it suggests that expanding the spectrum around the background of a state with a large time like $SL(2, R)$ charge in the BTZ sigma model results in a plane wave spectrum. It would be interesting to do this explicitly.

5 In-falling strings as local quenches

In this section, we show that the holographic duals of in-falling geodesics, circular strings, as well as magnons in the BTZ are local time-dependent quenches. These quenches are more general compared to those studied earlier in the literature in the AdS_3/CFT_2 context [15, 24–29]. We will see that the quenches here carry R-charges, marginal operators acquire non-trivial expectation values, and the left-moving and right-moving pulses of the quenches are not symmetric. In spite of the large amount of literature on local quenches, especially in the context of AdS_3/CFT_2 , such quenches have not been studied earlier. Let us first recall the AdS_3/CFT_2 dictionary for a particle of mass m at the origin of global AdS_3 [25]. The CFT_2 is on the cylinder parameterised by (t, ϕ) with $\phi \sim \phi + 2\pi$. At finite gravitational coupling G_N particle at the origin of AdS_3 backreacts and induces a conical defect. This can be seen by considering Einstein's equation ⁶

$$\hat{R}_{\mu\nu} - \frac{1}{2}g_{\mu\nu}\hat{R} - \frac{g_{\mu\nu}}{R^2} = 8\pi G_N T_{\mu\nu}, \quad (5.1)$$

where the only non-zero component of the stress tensor is given by

$$T^{tt} = \frac{m}{r}\delta(r)\delta(\phi). \quad (5.2)$$

We solve Einstein's equation and obtain the backreacted metric, which is the metric of the conical defect

$$ds^2 = -(r^2 + R^2 - \tilde{m})dt^2 + \frac{R^2}{r^2 + R^2 - \tilde{m}}dr^2 + r^2d\phi^2, \quad (5.3)$$

with

$$\tilde{m} = 8G_N R^2 m. \quad (5.4)$$

⁶We have used the \hat{R} to distinguish the Riemann curvature from the radius of curvature R of AdS_3 .

We can read out the stress tensor from the back-reacted geometry using the Fefferman-Graham expansion. This allows us to conclude that the state in the CFT_2 is created by the insertion of a primary operator \mathcal{O} at $t \rightarrow -\infty$ on the cylinder. The dimension of the operator and the mass of the particle are related by

$$m = \frac{\Delta_{\mathcal{O}}}{R}, \quad \tilde{m} = 8G_N R \Delta_{\mathcal{O}} = \frac{12\Delta_{\mathcal{O}} R^2}{c}. \quad (5.5)$$

To obtain the last equality, we have used the Brown-Henneaux formula

$$\frac{1}{G_N} = \frac{2c}{3R}. \quad (5.6)$$

Thus, the state in the CFT can be written as

$$|\mathcal{O}\rangle = \lim_{t \rightarrow -\infty} \mathcal{O}(t, 0) |0\rangle. \quad (5.7)$$

When this particle is in-falling in the BTZ geometry, it has been shown that the dual description of the back-reacted geometry is that of a local quench. The back-reacted geometry can be obtained by using the coordinate transformation (2.5) on the conical defect geometry (5.3). The state in the CFT is described by the density matrix

$$\begin{aligned} \rho_{\epsilon} &= \mathcal{N} e^{-itHt} \left(e^{-\epsilon H} \mathcal{O}(0, 0) e^{\epsilon H} \right) \rho_{\beta} \left(e^{-\epsilon H} \mathcal{O}^{\dagger}(0, 0) e^{\epsilon H} \right) e^{iHt}, \\ \rho_{\beta} &= e^{-\beta H}. \end{aligned} \quad (5.8)$$

Here ρ_{β} is the thermal density matrix of the dual CFT and $\mathcal{O}(0, 0)$ is the conformal primary field generating an excitation at $t = 0$, placed at the origin in the spatial direction in the thermal CFT. \mathcal{N} is introduced to normalise the density matrix. The expectation value of the stress tensor on this state is time-dependent. It starts out at $t = 0$ as a single pulse at the origin, splits into 2 symmetric left and right-moving pulses. These pulses travel at the speed of light. The height of the pulse is proportional to the operator dimension and therefore related to the mass of the in-falling particle in the dual geometry. The variable ϵ is the width of the pulse and can be shown to be related to the η_1 of the map (2.5), or to the radial position at which the particle is released using the initial conditions (2.18). Our subsequent discussion will review and generalise these facts about local quenches. From the results in sections 2, 3, we see that the in-falling geodesics, circular strings, and magnons follow the same trajectory in BTZ as massive geodesics. However, their mass arises due to the angular momenta in the compact S^3 . They also have velocity in the longitudinal direction. In this section, we show that the dual description of these in-falling classical solutions is local quenches as described earlier, in addition, they carry expectation values of R -charges due to the angular momentum in the S^3 and expectation values of scalars that arise from the dimensional reduction on S^3 . We show that these quenches are not symmetric pulses moving on the left and right light cones in the CFT_2 , the parameter η_2 in the map (2.43), which turns on velocity of the in falling particle in the BTZ renders the width as well as the height of the left moving and right moving pulse asymmetric. The

energy density profile of this quench is shown in Figure 1. In the dual thermal CFT, the dual state is the density matrix

$$\rho = \mathcal{N} e^{-iHt} \mathcal{O}(-i\epsilon_1, i\epsilon_2) \rho_\beta \mathcal{O}^\dagger(i\epsilon_1, -i\epsilon_2) e^{iHt}. \quad (5.9)$$

The ϵ_i are parameters which regularise the local quench, the quenches studied earlier in [15, 29] considered the situation with $\epsilon_1 = \epsilon_2$. ρ_β is the thermal density matrix and \mathcal{N} is the normalisation chosen to ensure $\text{Tr}(\rho^2) = 1$. We will show that the parameters ϵ_1, ϵ_2 in the CFT are related to the parameters η_1, η_2 of the maps of the in-falling particle (2.43). As far as we are aware, our study is the first instance of asymmetric quenches and that of embedding local quenches fully in the $AdS_3 \times S^3 \times M$ background.

To proceed, we first study the particle localised in the centre of AdS_3 carrying angular momentum along the S^3 and show that the dual description is that of a state in the CFT carrying R charge and expectation value of a marginal operator dual to the scalars that arise from the compactification on S^3 . We then generalise this observation to circular strings and giant magnons. This is done by obtaining the back-reacted geometry of these solutions and reading off the relevant R -charges and the expectation values. We then use the maps (2.5) and (2.43) to obtain the back-reacted geometry of in-falling geodesics, circular strings and magnons. This allows us to show that their dual description in the thermal CFT is as local quenches carrying R-charges and expectation values of marginal operators.

5.1 CFT duals of geodesics solutions in $AdS_3 \times S^3 \times M$

We begin by considering a point-like string solution localised at the origin of AdS_3 and rotating along one of the angular directions of S^3 . This is a BPS configuration for all M being T^4, K^3 or $S^3 \times S^1$. The world sheet couples to gravity via the action

$$S_P = \frac{k}{4\pi} \int d^{10}x \sqrt{G} \int d^2\sigma \left[G_{\mu\nu} \partial_a x^\mu \partial^a x^\nu \right] \frac{\delta(x^\mu - \bar{x}^\mu(\sigma))}{\sqrt{G}}. \quad (5.10)$$

Here μ, ν take values in $\{0, 1, \dots, 9\}$. To be specific, let us take the target space metric to be $AdS_3 \times S^3 \times T^4$, the discussion can be easily generalised to the other situations.

$$ds^2 = G_{\mu\nu} dx^\mu dx^\nu = ds_{AdS_3}^2 + R^2 ds_3^2 + ds_M^2. \quad (5.11)$$

where the metric on the AdS_3 and S^3 is given in (2.3), (3.7). The trajectory of the particle at the origin and spinning along the angle ϕ_2 of the sphere is given by

$$\begin{aligned} t(\sigma^0, \sigma^1) &= \kappa \sigma^0, & r(\sigma^0, \sigma^1) &= 0, & \phi(\sigma^0, \sigma^1) &= 0, \\ \psi(\sigma^0, \sigma^1) &= 0, & \phi_1(\sigma^0, \sigma^1) &= 0, & \phi_2(\sigma^0, \sigma^1) &= \frac{J}{k} \sigma^0, \\ X(\sigma^0, \sigma^1)|_M &= x_M = \text{constant}. \end{aligned} \quad (5.12)$$

The Virasoro condition, or the geodesic being massless, leads to the equality

$$\Delta = J, \quad \Delta = k\kappa. \quad (5.13)$$

The stress tensor sourced by this particle is obtained by the definition

$$T_{\mu\nu} = -\frac{2}{\sqrt{G}} \frac{\delta S_P}{\delta G^{\mu\nu}}. \quad (5.14)$$

The non-zero components of the 10-dimensional stress tensor are given by

$$\begin{aligned} T^{tt} &= \frac{\Delta}{R} \frac{\delta(r)\delta(\phi)}{r} \frac{\delta(\psi)\delta(\phi_1)\delta(\phi_2-t)}{\sqrt{g_{S^3}}} \frac{\delta^4(X_M - x_M)}{\sqrt{G_M}}, \\ T^{t\phi_2} &= \frac{\Delta}{R} \frac{\delta(r)\delta(\phi)}{r} \frac{\delta(\psi)\delta(\phi_1)\delta(\phi_2-t)}{\sqrt{g_{S^3}}} \frac{\delta^4(X_M - x_M)}{\sqrt{G_M}}, \\ T^{\phi_2\phi_2} &= \frac{\Delta}{R} \frac{\delta(r)\delta(\phi)}{r} \frac{\delta(\psi)\delta(\phi_1)\delta(\phi_2-t)}{\sqrt{g_{S^3}}} \frac{\delta^4(X_M - x_M)}{\sqrt{G_M}}. \end{aligned} \quad (5.15)$$

To arrive at these expressions, we have performed the integral over the world sheet coordinates and used $\Delta = J$. Note that all the non-zero components are proportional to Δ .

Let us dimensionally reduce these sources on $AdS_3 \times S^3$ and focus on the lowest Kaluza-Klein mode on the sphere S^3 . This can be done by integrating out the coordinates on $S^3 \times M$. Therefore, dimensional reduction of the stress tensor components in (5.15) on $S^3 \times M^3$, we obtain the following sources

$$\begin{aligned} \hat{T}^{tt} &= \frac{\Delta}{R} \frac{\delta(r)\delta(\phi)}{r}, \\ \hat{J}^t \equiv T^{t\phi_2} &= \frac{\Delta}{R} \frac{\delta(r)\delta(\phi)}{r}, \\ \hat{J}_\psi \equiv T^{\phi_2\phi_2} &= \frac{\Delta}{R} \frac{\delta(r)\delta(\phi)}{r}. \end{aligned} \quad (5.16)$$

The energy density T^{tt} is a source for the Einstein's equations in AdS_3 , the stress tensor component $T^{t\phi_2}$ is a source for a $U(1)$ gauge field A_μ in AdS_3 . Since this component of the stress tensor is the charge density for the $U(1)_R$ isometry of the S^3 , it should source the gauge field corresponding to this symmetry. In AdS_3 the R-symmetry gauge field obeys the Chern-Simons equations of motion [30, 31]⁷, therefore $T^{t\phi_2}$ sources a Chern-Simons gauge field. The component $T^{\phi_2\phi_2}$ sources a scalar ψ in AdS_3 . The scalar field ψ we choose to focus on is the dilaton in 6 dimensions, which is massless when compactified on $AdS_3 \times S^3$, see table (6.15) of [34]. The stress tensor $T^{\phi_2\phi_2}$ couples to the $G_{\phi_1\phi_1}$ component of the metric in the string frame; therefore, it would couple to the dilaton in 6 dimensions in the Einstein frame. From these considerations, the relevant dimensionally reduced effective action is given by

$$S = \frac{1}{16\pi G_N} \int d^3x \sqrt{g} \left(\hat{R} + \frac{2}{R^2} + \frac{R}{2} \frac{\epsilon^{\mu\nu\rho}}{\sqrt{g}} A_\mu \partial_\nu A_\rho - \partial_\mu \psi \partial^\mu \psi \right). \quad (5.17)$$

Here μ, ν, ρ take values along the AdS_3 directions and $\epsilon^{tr\phi} = 1$. The factor of R in front of the Chern-Simons is required since the level of the Chern-Simons is proportional to the

⁷See [32, 33] for the action obtained after dimensional reduction of gauged supergravity from 6 dimensions on $AdS_3 \times S^3$.

central charge by supersymmetry. The central charge is given by the Brown-Henneaux formula (5.6). Therefore we have

$$k_{\text{Chern Simons}} = \frac{c}{6} = \frac{R}{4G_N}. \quad (5.18)$$

The sources in (5.16) couple to the fields by the following interaction term

$$S_{\text{int}} = \int d^3x \sqrt{g} \left(-\frac{1}{2} T_{\mu\nu} \delta g^{\mu\nu} - J_\mu \delta A^\mu - \hat{J}_\psi \delta \psi \right). \quad (5.19)$$

This is obtained by dimensional reduction of the coupling of the relevant fluctuations to the higher-dimensional metric. Considering the action in (5.17) and the sources in (5.19), the dimensionally reduced equations of motion in AdS_3 become

$$\begin{aligned} \hat{R}_{\mu\nu} - \frac{1}{2} g_{\mu\nu} \hat{R} - g_{\mu\nu} &= 8\pi G_N \hat{T}_{\mu\nu}, \\ \frac{1}{\sqrt{g}} \epsilon^{\mu\nu\rho} \partial_\nu A_\rho &= 16\pi G_N \hat{J}^\nu, \\ \frac{1}{\sqrt{g}} \partial_\mu \left(\sqrt{g} g^{\mu\nu} \partial_\nu \psi \right) &= 8\pi G_N \hat{J}_\psi. \end{aligned} \quad (5.20)$$

G_N is Newton's constant in 3 dimensions. As we are interested in the backreacted solution to the leading order in G_N , we can ignore the stress tensor of the scalar in Einstein's equation. From the equations of motion of the scalar, we see that these fields are of the order G_N , and therefore they contribute at G_N^2 to the stress tensors. The Chern-Simons field does not contribute to the stress tensor. Therefore, the equations of motion are that for the metric, the Chern-Simons $U(1)$ field and a minimally coupled massless scalar ψ in the background of AdS_3 with their corresponding sources at the origin. The AdS/CFT duality relates metric fluctuations to the conserved stress tensor of the CFT and the gauge field in the bulk to a conserved $U(1)$ R current in the CFT. A minimally coupled scalar field of mass m in the bulk is dual to a primary operator Ψ , of conformal dimension Δ , which is given by

$$\Delta_\Psi = 1 + \sqrt{1 + m^2 R^2}. \quad (5.21)$$

Here we have specialised to the AdS_3/CFT_2 case. Thus, the massless scalar ψ in the bulk is dual to a marginal scalar operator Ψ with conformal dimension $\Delta_\Psi = 2$. Using AdS/CFT correspondence, we can read out the expectation value of the stress tensor and the $U(1)$ current. We will also show that the backreacted solution obtained by solving the equations in (5.20) turns on the expectation value of the boundary stress tensor, a background $U(1)$ charge, as well as an expectation value of the operator Ψ in the boundary CFT. We then show that such expectation values are non-zero for a state in the CFT created by an operator \mathcal{O} which has conformal dimension and $U(1)$ charge equal to Δ ⁸. In addition to this, the operator must have a non-trivial 3-point function with the marginal operator Ψ equal to Δ .

⁸ Δ is the strength of the sources in (5.16).

The backreacted solution of the spinning geodesic

The solution to Einstein's equation in (5.20) is known and is given by the conical defect metric

$$ds^2 = -(r^2 + R^2 - \tilde{m})dt^2 + \frac{R^2}{r^2 + R^2 - \tilde{m}}dr^2 + r^2d\phi^2, \quad (5.22)$$

with

$$\tilde{m} = 8G_N R \Delta. \quad (5.23)$$

Though this is an exact solution to Einstein's equation, as written in (5.20), we have neglected the stress tensor of the scalar and the photon in the equation; therefore, the above solution is the leading order solution in G_N . We now solve the equations of motion for the scalar field in (5.20). It is clear that to obtain the scalar field at the leading order in G_N , we can assume the background metric to be AdS_3 . Since the source is radially symmetric, the scalar field only depends on the coordinate r . The Laplacian on AdS_3 reduces to

$$\frac{1}{rR}\partial_r[rR(r^2 + R^2)\partial_r\psi] = 8\pi G_N \frac{\Delta}{Rr}\delta(r)\delta(\phi). \quad (5.24)$$

Solving for ψ , we obtain

$$\psi = C + \frac{2\Delta G_N}{R} \log\left(\frac{r^2}{r^2 + R^2}\right). \quad (5.25)$$

We can set $C = 0$ by requiring the solution to be normalizable at $r \rightarrow \infty$. Thus we have

$$\begin{aligned} \psi &= \frac{2\Delta G_N}{R} \log\left(\frac{r^2}{r^2 + R^2}\right) \\ &= -\frac{2\Delta G_N}{R} \frac{R^2}{r^2} + \dots \end{aligned} \quad (5.26)$$

Observe that the scalar field falls off at the boundary as $\frac{R^2}{r^2}$, which is the expected fall-off behaviour for the expectation value of the dual operator Ψ of dimension 2. To solve for the gauge field, since we have an electric charge at the origin of AdS_3 . This sources a magnetic field strength of the Chern-Simons field in the angular direction. We choose a gauge so that only the component A_ϕ is non-zero. We obtain the equations

$$\frac{1}{rR}\partial_r A_\phi = \frac{16\pi G_N}{R} \frac{\Delta}{Rr}\delta(r)\delta(\phi). \quad (5.27)$$

Therefore, the solution A_ϕ is a constant whose value is fixed by the Stokes theorem

$$A_\phi = 8\pi G_N \frac{\Delta}{R}. \quad (5.28)$$

Reading out the expectation value of the boundary operators

Now that we have the backreacted solution, we obtain the expectation values of the boundary operators. We can read out the stress tensor expectation value in the CFT by writing the metric in the Fefferman-Graham form. We briefly summarise this for convenience. First, we expand the asymptotically AdS_3 metric in (5.22) as follows

$$ds^2 = \frac{R^2}{z^2} (dz^2 + g_{ij}(z, x)dx^i dx^j), \quad (5.29)$$

then in general g_{ij} takes the form

$$g_{ij}(z, x) = g_{ij}^{(0)} + z^2 g_{ij}^{(2)} + h_{ij} z^2 \log\left(\frac{z^2}{R^2}\right) + O(z^3). \quad (5.30)$$

The expectation of the stress tensor of the boundary CFT is given by

$$\langle T_{ij} \rangle_{\text{FG}, AdS_3} = \frac{R}{4G_N} g_{ij}^{(2)}. \quad (5.31)$$

Carrying this calculation on the metric in (5.22) leads to the following non-vanishing components for the expectation value of the boundary stress tensor

$$\begin{aligned} \langle T_{tt} \rangle_{\text{FG}, AdS_3} &= -\frac{R}{4G_N} \frac{R^2 - \tilde{m}}{2R^4} \\ &= \frac{\Delta}{R^2} - \frac{c}{12R^2} \\ &= \langle T_{\phi\phi} \rangle_{\text{FG}, AdS_3}. \end{aligned} \quad (5.32)$$

To obtain the second line, we have used (5.5) and the Brown-Henneaux formula (5.6). In Fefferman-Graham coordinates, the $U(1)$ gauge field takes the form [35]

$$\lim_{z \rightarrow 0} A_\mu(z, x) = A_\mu^{(0)}(x) + z^2 A_\mu^{(2)}(x) + \dots \quad (5.33)$$

We evaluate the expectation value of the charge density and current by using the holographic formula [35]

$$\langle j^t \rangle_{AdS_3} = \frac{1}{8G_N} A_t^{(0)}, \quad \langle j^\phi \rangle_{AdS_3} = \frac{1}{8G_N} A_\phi^{(0)}. \quad (5.34)$$

We have removed the factor of R , which occurs in the numerator, so that the gauge fields are restored to their canonical dimension of one in the action (5.17). Observe that the gauge fields A_t, A_ϕ in the action are dimensionless. Reading out the expectation value of the charge density and current using the solution (5.28) and (5.34), we obtain

$$\langle j^t \rangle_{AdS_3} = 0, \quad \langle j^\phi \rangle_{AdS_3} = \frac{\Delta}{R}. \quad (5.35)$$

The expectation value of the scalar operator Ψ of conformal dimension $\Delta_\Psi = 2$ is obtained by reading out the fall off behaviour in the dual scalar field ψ in (5.26)

$$\lim_{r \rightarrow \infty} \psi(r) = \psi_0 + \psi_1 \frac{R^2}{r^2} + \dots \quad (5.36)$$

then ⁹

$$\langle \Psi \rangle_{\text{AdS}_3} = (2\Delta_\Psi - 2) \frac{R}{4G_N} \frac{\psi_1}{R^2}. \quad (5.37)$$

Reading out ψ_1 from the solution in (5.26) and using (5.37) we obtain

$$\langle \Psi \rangle_{\text{AdS}_3} = -\frac{\Delta}{R^2}. \quad (5.38)$$

The CFT dual of the backreacted solution

From the expectation values of the stress tensor, the $U(1)$ current and the marginal operator Ψ in (5.32), (5.35) and (5.38), obtained from the back reacted solution, it is clear that the CFT is in an excited state with a scalar operator \mathcal{O} of conformal dimension $\Delta_\mathcal{O} = \Delta$. To confirm this, we evaluate the following expectation value of the state created by inserting the operator \mathcal{O} on the cylinder at $t \rightarrow -\infty$. One approach to do this would be to evaluate the expectation values in the Euclidean cylinder and use the transformation

$$z_{\text{plane}} = \exp\left(-i\frac{w}{R}\right), \quad w = \phi + i\tau, \quad (5.39)$$

and then transform to the Minkowski theory by taking $\tau = it$. Note that the cylinder is of radius R . Performing this, we obtain

$$\begin{aligned} \frac{\langle \mathcal{O} | T_{tt}(0,0) | \mathcal{O} \rangle}{\langle \mathcal{O} | \mathcal{O} \rangle} &= -\frac{\langle \mathcal{O} | T_{ww}(0) + T_{\bar{w}\bar{w}}(0) | \mathcal{O} \rangle}{\langle \mathcal{O} | \mathcal{O} \rangle} \\ &= \frac{\Delta}{R^2} - \frac{c}{12R^2}. \end{aligned} \quad (5.40)$$

The shift by the central charge occurs due to the Schwarzian in the transformation of the stress tensor from the plane to the cylinder. The left and right conformal dimensions of the scalar operator are the same and equal to $\frac{\Delta}{2}$. Since the left and right weights are the same, we get

$$\frac{\langle \mathcal{O} | T_{\phi\phi}(0,0) | \mathcal{O} \rangle}{\langle \mathcal{O} | \mathcal{O} \rangle} = \frac{\langle \mathcal{O} | T_{zz}(0) - T_{\bar{z}\bar{z}}(0) | \mathcal{O} \rangle}{\langle \mathcal{O} | \mathcal{O} \rangle} = 0. \quad (5.41)$$

Let the scalar operator be charged under a $U(1)$ conserved current in the CFT with charges $(\frac{\Delta}{2}, \frac{\Delta}{2})$ both for the left and right moving $U(1)$ currents, we obtain

$$\begin{aligned} \frac{\langle \mathcal{O} | j_t(0,0) | \mathcal{O} \rangle}{\langle \mathcal{O} | \mathcal{O} \rangle} &= -i \frac{\langle \mathcal{O} | j_w(0) - j_{\bar{w}}(0) | \mathcal{O} \rangle}{\langle \mathcal{O} | \mathcal{O} \rangle} \\ &= 0. \end{aligned} \quad (5.42)$$

Similarly, we have

$$\begin{aligned} \frac{\langle \mathcal{O} | j_\phi(0,0) | \mathcal{O} \rangle}{\langle \mathcal{O} | \mathcal{O} \rangle} &= \frac{\langle \mathcal{O} | j_w(0) + j_{\bar{w}}(0) | \mathcal{O} \rangle}{\langle \mathcal{O} | \mathcal{O} \rangle} \\ &= \frac{\Delta}{R} \end{aligned} \quad (5.43)$$

⁹It is conventional to define the coordinate $z = R^2/r$ and read out the coefficient of z^{Δ_Ψ} as the expectation value of the dual operator. This explains the additional factor of $1/R^2$ in (5.37) which results in the correct scaling behaviour for the expectation value.

Now the expectation value of the marginal operator Ψ in the state $|\mathcal{O}\rangle$ is given by

$$\frac{\langle \mathcal{O}|\Psi(0,0)|\mathcal{O}\rangle}{\langle \mathcal{O}|\mathcal{O}\rangle} = \frac{C_{\mathcal{O}\mathcal{O}\Psi}}{R^2}. \quad (5.44)$$

where $C_{\mathcal{O}\mathcal{O}\Psi}$ is the OPE coefficient of these operators. Comparing with the result for the expectation value from holography in (5.38) allows us to identify the 3 point function as

$$C_{\mathcal{O}\mathcal{O}\Psi} = -\Delta. \quad (5.45)$$

5.2 In falling spinning geodesics in $BTZ \times S^3 \times M$ as quenches

The CFT dual to the BTZ geometry is a thermal CFT; therefore, we would expect the geometry with in-falling geodesics or strings into the BTZ to be excitations in the thermal CFT. We would like to identify these excitations in the thermal CFT. In this section, we first construct the backreacted geometry of the in-falling geodesic in BTZ and spinning on S^3 and then use it to find the expectation values of the stress tensor, the $U(1)$ current and the marginal operator in the dual thermal CFT. We have shown that the coordinate transformation (2.43) takes the particle at the origin of AdS_3 and spinning on S^3 to an in-falling geodesic in BTZ and spinning on S^3 . Therefore, we use this coordinate transformation on the backreacted solution of the particle spinning particle at the origin of AdS_3 given in equations (5.22), (5.26), (5.22) to obtain the backreacted solution of the particle in falling in the BTZ background. It is convenient to work with the following re-definition of the radial coordinate

$$\rho = \frac{1}{z}. \quad (5.46)$$

Now the radial coordinate z has the dimensions of length, since ρ has dimensions of mass. The BTZ metric then becomes

$$ds^2 = \frac{R^2}{z^2} \left[- (1 - M^2 z^2) d\tau^2 + \frac{dz^2}{1 - M^2 z^2} + dx^2 \right]. \quad (5.47)$$

Since we are interested in the background at the leading order in G_N , we can proceed by expanding this conical defect metric (5.22) to the leading order

$$ds^2 = -(r^2 + R^2) dt^2 + \frac{R^2}{r^2 + R^2} dt^2 + r^2 d\phi^2 + \delta g_{\mu\nu} dx^\mu dx^\nu, \quad (5.48)$$

$$\delta g_{\mu\nu} dx^\mu dx^\nu = \tilde{m} \left(dt^2 + \frac{R^2}{(r^2 + R^2)^2} dr^2 \right).$$

To make the transformation to the BTZ, we use the relation of the AdS_3 coordinates to the embedding space given in (2.43) and write

$$dt^2 = \left(\frac{X_0 dX_1 - X_1 dX_0}{X_0^2 + X_1^2} \right)^2, \quad (5.49)$$

$$\frac{R^2}{(r^2 + R^2)^2} dr^2 = \frac{R^2 (X_2 dX_2 + X_3 dX_3)^2}{(X_0^2 + X_1^2)^2 (X_2^2 + X_3^2)}.$$

In this form, the perturbative corrections can be easily converted to the BTZ co-ordinates using the relation (2.43). The result is the backreacted metric of an in-falling particle in BTZ. This metric can be expanded near the boundary and it of the form

$$ds^2 = \frac{R^2}{z^2} \left[- (1 - M^2 z^2) d\tau^2 + \frac{dz^2}{1 - M^2 z^2} + dx^2 \right] + \delta g_{zz}(\tau x) dz^2 + \delta g_{\tau\tau}(\tau, x) d\tau^2 + \delta g_{xx}(\tau, x) dx^2 + \delta g_{\tau x}(\tau, x) d\tau dx + \mathcal{O}(z). \quad (5.50)$$

Observe that the background AdS_3 in (5.48) gets converted to BTZ, while the correction proportional to \tilde{m} will be written as the back reaction to the BTZ background. The expressions for the perturbation are long and cumbersome, but as we have kept the leading order at the boundary, whose boundary coordinates are τ, x . We can now go over to Fefferman-Graham coordinates and read out the expectation value of the boundary stress tensor. This is given by

$$\begin{aligned} \langle T_{\tau\tau} \rangle_{\text{FG}} &= \frac{R}{4G_N} \left(\frac{M^2}{2} - \frac{\delta g_{zz}}{2R^2} + \frac{\delta g_{\tau\tau}}{R^2} \right), \\ \langle T_{xx} \rangle_{\text{FG}} &= \frac{R}{4G_N} \left(\frac{M^2}{2} + \frac{\delta g_{zz}}{2R^2} + \frac{\delta g_{xx}}{R^2} \right), \\ \langle T_{\tau x} \rangle_{\text{FG}} &= \frac{1}{4G_N R} \delta g_{\tau z}. \end{aligned} \quad (5.51)$$

Substituting the perturbations, we obtain

$$\begin{aligned} \langle T_{\tau\tau} \rangle_{\text{FG}} &= \langle T_{xx} \rangle_{\text{FG}} \\ &= \frac{M^2 R}{8G_N} + \frac{\tilde{m} M^2}{16G_N R} \left\{ \frac{1}{[\cosh M(x + \tau) \cosh(\eta_1 - \eta_2) - \sinh(\eta_1 - \eta_2)]^2} \right. \\ &\quad \left. + \frac{1}{[\cosh M(x - \tau) \cosh(\eta_1 + \eta_2) - \sinh(\eta_1 + \eta_2)]^2} \right\}, \end{aligned} \quad (5.52)$$

$$\begin{aligned} \langle T_{\tau x} \rangle_{\text{FG}} &= \frac{\tilde{m} M^2}{16G_N R} \left\{ \frac{1}{[\cosh M(x + \tau) \cosh(\eta_1 - \eta_2) - \sinh(\eta_1 - \eta_2)]^2} \right. \\ &\quad \left. - \frac{1}{[\cosh M(x - \tau) \cosh(\eta_1 + \eta_2) - \sinh(\eta_1 + \eta_2)]^2} \right\}. \end{aligned} \quad (5.53)$$

The expectation value of the stress tensor is conserved and traceless. The mass of BTZ is related to its temperature by

$$M = \frac{2\pi}{\beta}. \quad (5.54)$$

We can use this relation and the Brown-Henneaux formula in (5.6) to write these expectation values as

$$\begin{aligned} \langle T_{\tau\tau} \rangle_{\text{FG}} &= \langle T_{xx} \rangle_{\text{FG}} \\ &= \frac{c \pi^2}{3 \beta^2} + \frac{\Delta}{2} \left(\frac{2\pi}{\beta} \right)^2 \left\{ \frac{1}{\left[\cosh \frac{2\pi}{\beta} (x + \tau) \cosh (\eta_1 - \eta_2) - \sinh (\eta_1 - \eta_2) \right]^2} \right. \\ &\quad \left. + \frac{1}{\left[\cosh \frac{2\pi}{\beta} (x - \tau) \cosh (\eta_1 + \eta_2) - \sinh (\eta_1 + \eta_2) \right]^2} \right\}, \end{aligned} \quad (5.55)$$

$$\begin{aligned} \langle T_{\tau x} \rangle_{\text{FG}} &= \frac{\Delta}{2} \left(\frac{2\pi}{\beta} \right)^2 \left\{ \frac{1}{\left[\cosh \frac{2\pi}{\beta} (x + \tau) \cosh (\eta_1 - \eta_2) - \sinh (\eta_1 - \eta_2) \right]^2} \right. \\ &\quad \left. - \frac{1}{\left[\cosh \frac{2\pi}{\beta} (x - \tau) \cosh (\eta_1 + \eta_2) - \sinh (\eta_1 + \eta_2) \right]^2} \right\}. \end{aligned} \quad (5.56)$$

In Figure 1, we have plotted the expectation value of the energy density of the quench at instances of time. The pulse splits asymmetrically and quenches travel at the speed of light. For $\eta_1 \gg 1, \eta_2 \sim 1$, the height of the energy densities of the pulses is approximately given by

$$\begin{aligned} \text{Height of pulse 1} &\sim \frac{\Delta}{2} \left(\frac{2\pi}{\beta} \right)^2 e^{2(\eta_1 - \eta_2)}, \\ \text{Height of pulse 2} &\sim \frac{\Delta}{2} \left(\frac{2\pi}{\beta} \right)^2 e^{2(\eta_1 + \eta_2)}. \end{aligned} \quad (5.57)$$

To get an idea of the width of the pulses, it is convenient to take the limit $\beta \gg x, \tau$ and $\eta_1 \gg 1, \eta \sim 1$, then the widths of the two pulses are given by

$$\begin{aligned} \text{Width of pulse 1} &\sim \frac{\beta}{2\pi} e^{-(\eta_1 - \eta_2)}, \\ \text{Width of pulse 2} &\sim \frac{\beta}{2\pi} e^{-(\eta_1 + \eta_2)}. \end{aligned} \quad (5.58)$$

Therefore, the taller pulse is narrower than the smaller one, which can be clearly seen in the figure 1.

We now evaluate the expectation value of the $U(1)$ current in the backreacted geometry of the in-falling geometry. For this, it is convenient to use the coordinate transformation of the background gauge field found for the particle in AdS_3 to BTZ from (2.43) directly. This transformation is given by

$$\begin{aligned} t &= \arctan \left[\frac{\sqrt{\rho^2 - M^2} \sinh(M\tau) \cosh \eta_2 - \rho \sinh \eta_2 \sinh(Mx)}{\rho \cosh \eta_1 \cosh(Mx) - \sqrt{\rho^2 - M^2} \cosh(M\tau) \sinh \eta_1} \right], \\ \phi &= \arctan \left[\frac{\rho \sinh(Mx) \cosh \eta_2 - \sqrt{\rho^2 - M^2} \sinh(M\tau) \sinh \eta_2}{\sqrt{\rho^2 - M^2} \cosh(M\tau) \cosh \eta_1 - \rho \sinh \eta_1 \cosh(Mx)} \right], \\ r &= \frac{R}{M} \left[(\rho \sinh(Mx) \cosh \eta_2 - \sqrt{\rho^2 - M^2} \sinh(M\tau) \sinh \eta_2)^2 \right. \\ &\quad \left. + (\sqrt{\rho^2 - M^2} \sinh(M\tau) \cosh \eta_2 - \rho \sinh \eta_2 \sinh(Mx))^2 \right]^{\frac{1}{2}}. \end{aligned} \quad (5.59)$$

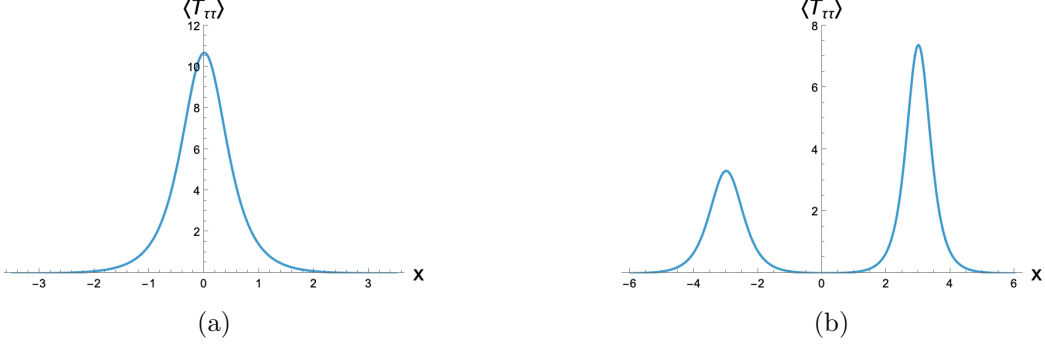


Figure 1: Expectation value of the energy density of the local quench. Panel (a) shows $\langle T_{\tau\tau} \rangle - \frac{c\pi^2}{3\beta^2}$ at $\tau = 0$, while panel (b) shows it at $\tau = 3$. Both plots are generated for the parameter values $\Delta = 2$, $\eta_1 - \eta_2 = 0.6$, and $\eta_1 + \eta_2 = 1$ with $\frac{2\pi}{\beta} = 1$. The profile initially consists of a single pulse, which subsequently splits into two pulses propagating at the speed of light. The height and width of the pulses are controlled by the parameters η_1 , η_2 , and the conformal dimension Δ of the primary operator. The pulses become symmetric when $\eta_2 = 0$.

Using these transformation we can use the field strength of the backreacted solution in AdS_3 in (5.28) to obtain the expectation value charge density at the boundary of the BTZ background. This results in

$$\begin{aligned} \langle j_\tau \rangle_{\text{BTZ}} &= \lim_{\rho \rightarrow \infty} \frac{R}{8G_N} A_\tau = \lim_{\rho \rightarrow \infty} \frac{R}{8G_N} \frac{\partial \phi}{\partial \tau} A_\phi & (5.60) \\ &= \frac{\Delta M}{2} \left[\frac{1}{\cosh M(x + \tau) \cosh(\eta_1 - \eta_2) - \sinh(\eta_1 - \eta_2)} - \frac{1}{\cosh M(x - \tau) \cosh(\eta_1 + \eta_2) - \sinh(\eta_1 + \eta_2)} \right] \\ &= \frac{\Delta}{2} \frac{2\pi}{\beta} \left[\frac{1}{\cosh \frac{2\pi}{\beta}(x + \tau) \cosh(\eta_1 - \eta_2) - \sinh(\eta_1 - \eta_2)} - \frac{1}{\cosh \frac{2\pi}{\beta}(x - \tau) \cosh(\eta_1 + \eta_2) - \sinh(\eta_1 + \eta_2)} \right]. \end{aligned}$$

In the second line, we have written the expression in terms of the temperature of the BTZ background. In BTZ coordinates, the gauge field had dimensions of inverse length; therefore, there is an additional factor of R along with G_N as compared to (5.34), which makes the overall factor the level of the Chern-Simons field as expected.¹⁰ Similarly, the spatial component of the current is given by

$$\begin{aligned} \langle j_x \rangle_{\text{BTZ}} &= \lim_{\rho \rightarrow \infty} \frac{R}{8G_N} A_x = \lim_{\rho \rightarrow \infty} \frac{R}{8G_N} \frac{\partial \phi}{\partial x} A_\phi & (5.61) \\ &= \frac{\Delta M}{2} \left[\frac{1}{\cosh M(x + \tau) \cosh(\eta_1 - \eta_2) - \sinh(\eta_1 - \eta_2)} + \frac{1}{\cosh M(x - \tau) \cosh(\eta_1 + \eta_2) - \sinh(\eta_1 + \eta_2)} \right] \\ &= \frac{\Delta}{2} \frac{2\pi}{\beta} \left[\frac{1}{\cosh \frac{2\pi}{\beta}(x + \tau) \cosh(\eta_1 - \eta_2) - \sinh(\eta_1 - \eta_2)} + \frac{1}{\cosh \frac{2\pi}{\beta}(x - \tau) \cosh(\eta_1 + \eta_2) - \sinh(\eta_1 + \eta_2)} \right]. \end{aligned}$$

In figures 2, 3, we have plotted the profile of the charge density and the current at two instances of time. From $\tau = 0$, the pulse splits into two and travels at the speed of light.

¹⁰Recall the coordinate t in AdS_3 is dimensionless while the coordinate τ in BTZ has the dimensions of length.

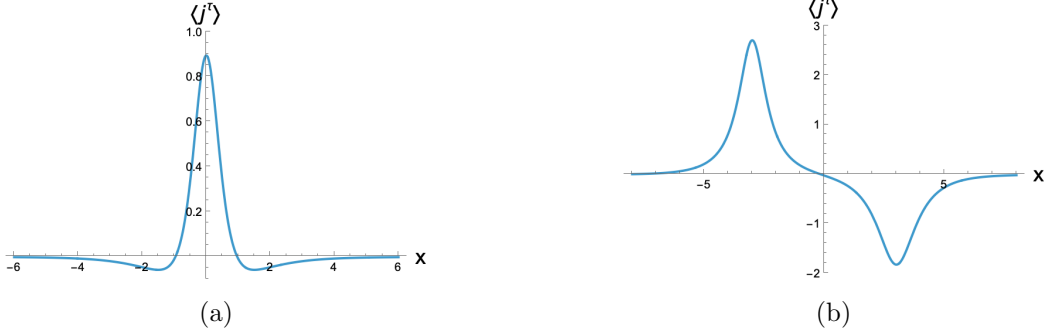


Figure 2: Profile of the expectation value of the charge at different times. Panel (a) shows $\langle j^\tau \rangle$ at $\tau = 0$, while panel (b) shows $\langle j^\tau \rangle$ at $\tau = 3$. Both plots are generated for $\Delta = 2$, $\eta_1 - \eta_2 = 1$, and $\eta_1 + \eta_2 = 0.6$ with $\frac{2\pi}{\beta} = 1$. Here, we have interchanged the value of the parameters so that the pulse at $\tau = 0$ is mostly positive. The qualitative behaviour of the profile remains the same as in the case of the energy density. The height and width of the pulses are determined by the parameters η_1 , η_2 , and the conformal dimension Δ of the primary operator.

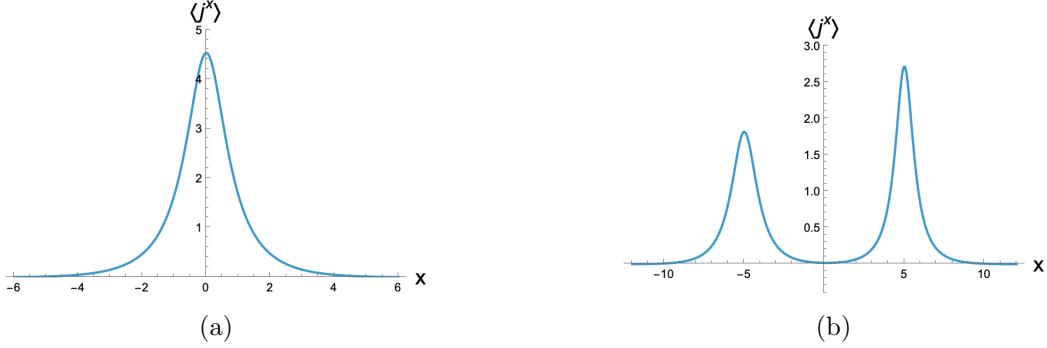


Figure 3: Profile of the expectation value of the current at different times. Panel (a) shows $\langle j^x \rangle$ at $\tau = 0$, while panel (b) shows $\langle j^x \rangle$ at $\tau = 5$ with $\frac{2\pi}{\beta} = 1$. Both plots are generated for $\Delta = 2$, $\eta_1 - \eta_2 = 0.6$, and $\eta_1 + \eta_2 = 1$. The qualitative behaviour of the profile remains the same as in the previous cases.

The quenches are asymmetric with their widths determined as given in equation (5.58). The heights of both the charge density and current quenches are given by

$$|\text{Height of pulse 1}| \sim \frac{\Delta}{2} \left(\frac{2\pi}{\beta} \right) e^{(\eta_1 - \eta_2)}, \quad |\text{Height of pulse 2}| \sim \frac{\Delta}{2} \left(\frac{2\pi}{\beta} \right) e^{(\eta_1 + \eta_2)},$$

for $\eta_1 \gg 1$, $\eta_2 \sim 1$. (5.62)

The profile of the scalar ψ in the backreacted geometry of the in-falling particle is found by using the coordinate transformation in (5.59) on the solution of the scalar given in (5.26), which results in

$$\lim_{\rho \rightarrow \infty} \psi(\rho, \tau, x) = \psi_0 + \frac{1}{\rho^2} \psi_1(\tau, x) + \dots \quad (5.63)$$

The expectation value of the marginal operator Ψ dual to the minimally coupled scalar ψ sourced by the in-falling particle is given by

$$\langle \Psi \rangle_{\text{BTZ}} = (2\Delta_\Psi - 2) \frac{R}{4G_N} \psi_1(\tau, x). \quad (5.64)$$

Note that ψ_1 has the dimensions of inverse length squared. Substituting the change of co-ordinates in (5.59) and extracting the coefficient $\psi_1(\tau, x)$, we obtain

$$\begin{aligned} & \langle \Psi \rangle_{\text{BTZ}} & (5.65) \\ &= \frac{-\Delta M^2}{\{\cosh M(x + \tau) \cosh(\eta_1 - \eta_2) - \sinh(\eta_1 - \eta_2)\} \{\cosh M(x - \tau) \cosh(\eta_1 + \eta_2) - \sinh(\eta_1 + \eta_2)\}} \\ &= \frac{-\Delta(\frac{2\pi}{\beta})^2}{\left\{ \cosh \frac{2\pi}{\beta}(x + \tau) \cosh(\eta_1 - \eta_2) - \sinh(\eta_1 - \eta_2) \right\} \left\{ \cosh \frac{2\pi}{\beta}(x - \tau) \cosh(\eta_1 + \eta_2) - \sinh(\eta_1 + \eta_2) \right\}}. \end{aligned}$$

In figure 4, we have plotted the expectation value of the scalar operator $|\langle \Psi \rangle|$ at 2 instances of time. The expectation value at initial time $\tau = 0$ is peaked at the origin, and then the peak moves away from the origin at the speed of light. The peak at time $\tau \gg \beta$ is approximately given by the expression

$$|\langle \Psi \rangle|_{\text{maximum}} \sim \Delta \left(\frac{2\pi}{\beta} \right)^2 e^{(-\frac{4\pi}{\beta}\tau + \eta_1 + \eta_2)}. \quad (5.66)$$

Thus, the height of the quench decreases in time. The width of the pulse for $\beta \gg \tau, x; \eta_1 \gg 1; \eta_2 \sim 1$ is given by

$$\text{Width of scalar expectation} \sim \frac{\beta}{2\pi} e^{-(\eta_1 + \eta_2)}. \quad (5.67)$$

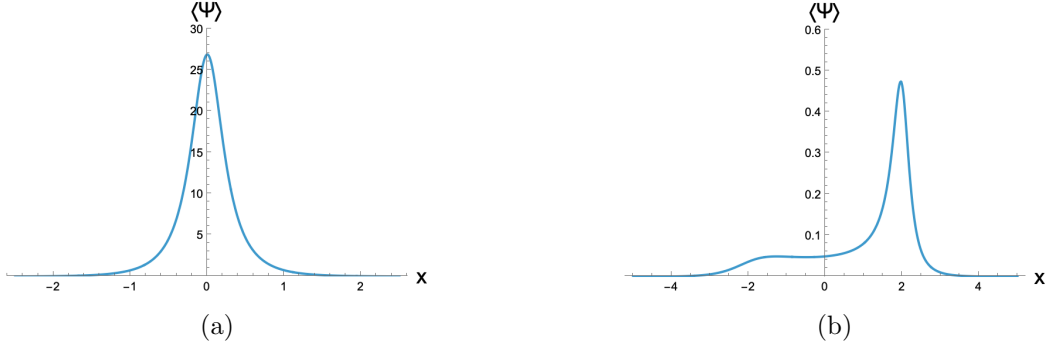


Figure 4: Expectation value of the negative of scalar operator Ψ . Panel (a) shows $\langle \Psi \rangle$ at $\tau = 0$, while panel (b) shows $\langle \Psi \rangle$ at $\tau = 2$. Both plots are generated for $\Delta = 2$, $\eta_1 + \eta_2 = 2$, and $\eta_1 - \eta_2 = 0.6$. Note the qualitative contrast between these profiles and those shown in the previous figures. The profile initially consists of a single pulse at all times, though its amplitude decreases and the peak shifts either to the left or to the right depending on the parameter values. For the parameters chosen here, the peak shifts to the right.

The density matrix of the in-falling particle in the thermal CFT

The CFT dual to the BTZ black hole is a thermal CFT. Therefore, the dual description of the in-falling particle should be an excitation on the thermal density matrix of the CFT. We consider the following state described by a density matrix for the dual description of the in-falling geodesic in the BTZ background

$$\rho = \mathcal{N} e^{-iHt} \mathcal{O}(w_1, \bar{w}_1) \rho_\beta \mathcal{O}^\dagger(w_2, \bar{w}_2) e^{iHt}, \quad (5.68)$$

where $\rho_\beta = e^{-\beta H}$ is the thermal density matrix and the normalisation \mathcal{N} is chosen so that $\text{Tr}\rho = 1$. The position coordinates of the operator are given by

$$w_1 = -i\epsilon_1, \quad w_2 = i\epsilon_1, \quad \bar{w}_1 = i\epsilon_2, \quad \bar{w}_2 = -i\epsilon_2 \quad (5.69)$$

with ϵ_i real. Such excitations are the generalisations of local quenches considered in [15, 29] for which the parameters ϵ_i were restricted to $\epsilon_1 = \epsilon_2$. These parameters determine the width of the local quenches. The coordinates of the operators are labelled in Lorentzian signature on the cylinder are

$$(w, \bar{w}) \equiv (x - \tau, x + \tau). \quad (5.70)$$

The Lorentzian co-ordinates can naturally be continued to Euclidean when $\tau \rightarrow -i\tau_E$. We take the operator \mathcal{O} to have conformal dimensions $(\frac{\Delta}{2}, \frac{\Delta}{2})$, with $U(1)$ charges $(\frac{\Delta}{2}, \frac{\Delta}{2})$. It also has a non-zero 3 point function with the marginal operator Ψ given by (5.45). We proceed to evaluate the expectation value of the energy density in the density matrix (5.68),

$$\begin{aligned} \langle T_{\tau\tau} \rangle_{CFT} &= \text{Tr}[\rho T_{tt}(x - \tau, x + \tau)], \\ &= \frac{\langle \mathcal{O}^\dagger(w_2, \bar{w}_2) T_{tt}(x - \tau, x + \tau) \mathcal{O}(w_1, \bar{w}_1) \rangle_\beta}{\langle \mathcal{O}^\dagger(w_4, \bar{w}_4) \mathcal{O}(w_1, \bar{w}_1) \rangle_\beta}. \end{aligned} \quad (5.71)$$

We use the map from the thermal cylinder to the plane, which is given by

$$z = \exp\left(\frac{2\pi}{\beta}w\right), \quad w = x + i\tau_E, \quad \tau_E = i\tau \quad (5.72)$$

to obtain thermal expectation values. This results in

$$\langle T_{\tau\tau} \rangle_{CFT} = \frac{\pi^2 c}{3\beta^2} - \frac{4\pi^2}{\beta^2} \left[z^2 \frac{\langle \mathcal{O}^\dagger(z_2, \bar{z}_2) T(z) \mathcal{O}(z_1, \bar{z}_1) \rangle_\beta}{\langle \mathcal{O}^\dagger(z_2, \bar{z}_2) \mathcal{O}(z_1, \bar{z}_1) \rangle_\beta} + \bar{z}^2 \frac{\langle \mathcal{O}^\dagger(z_2, \bar{z}_2) \bar{T}(\bar{z}) \mathcal{O}(z_1, \bar{z}_1) \rangle_\beta}{\langle \mathcal{O}^\dagger(z_2, \bar{z}_2) \mathcal{O}(z_1, \bar{z}_1) \rangle_\beta} \right]. \quad (5.73)$$

To obtain this expression, we have used the transformation of the cylinder to the plane, which results in the Schwarzian contribution along with the three-point function of the stress tensor with the two primaries. The three-point function is determined by the stress tensor Ward identity. Here we need to substitute the coordinates on the plane in terms of the cylinder using the map (5.72). This results in

$$\langle T_{\tau\tau} \rangle_{CFT} = \frac{\pi^2 c}{3\beta^2} + \frac{4\pi^2 \Delta}{2\beta^2} \left[\frac{\sin^2 \frac{2\pi\epsilon_1}{\beta}}{\left\{ \cosh \frac{2\pi}{\beta}(x + \tau) - \cos \frac{2\pi\epsilon_1}{\beta} \right\}^2} + \frac{\sin^2 \frac{2\pi\epsilon_2}{\beta}}{\left\{ \cosh \frac{2\pi}{\beta}(x - \tau) - \cos \frac{2\pi\epsilon_2}{\beta} \right\}^2} \right]. \quad (5.74)$$

On comparing the boundary stress expectation value obtained from the backreacted geometry of the in-falling particle in (5.55) and the above expectation value of the stress tensor in the state (5.68), we see that upon making the identifications

$$\tanh(\eta_1 - \eta_2) = \cos \frac{2\pi\epsilon_1}{\beta}, \quad \tanh(\eta_2 + \eta_1) = \cos \frac{2\pi\epsilon_2}{\beta}, \quad (5.75)$$

they precisely agree. We can repeat the same calculation in the CFT for the expectation value $\langle T_{\tau x} \rangle_{CFT}$, and it too agrees with (5.56) upon the identifications (5.75). Let us proceed to the expectation value of the charge density. We obtain

$$\begin{aligned} \langle j_\tau \rangle_{CFT} &= \text{Tr}[\rho j_t(x - \tau, x + \tau)], \\ &= -i \left[\frac{\langle \mathcal{O}^\dagger(w_2, \bar{w}_2) j(w) \mathcal{O}(w_1, \bar{w}_1) \rangle_\beta}{\langle \mathcal{O}^\dagger(w_2, \bar{w}_2) \mathcal{O}(w_1, \bar{w}_1) \rangle_\beta} - \frac{\langle \mathcal{O}^\dagger(w_2, \bar{w}_2) \bar{j}(\bar{w}) \bar{\mathcal{O}}(w_1, \bar{w}_1) \rangle_\beta}{\langle \mathcal{O}^\dagger(w_2, \bar{w}_2) \bar{\mathcal{O}}(w_1, \bar{w}_1) \rangle_\beta} \right]. \end{aligned} \quad (5.76)$$

We can evaluate the first three-point function using the fact that the holomorphic current is a dimension $(1, 0)$ operator and the operator \mathcal{O} has the holomorphic charge $\frac{\Delta}{2}$ and using the cylinder to plane map. A similar approach can be done for the anti-holomorphic three-point function. This results in the following expectation value

$$\langle j_\tau \rangle_{CFT\beta} = \frac{\Delta}{2} \frac{2\pi}{\beta} \left[\frac{\sin \frac{2\pi}{\beta} \epsilon_1}{\cosh \frac{2\pi}{\beta} (x + \tau) - \cos \frac{2\pi}{\beta} \epsilon_1} - \frac{\sin \frac{2\pi}{\beta} \epsilon_2}{\cosh \frac{2\pi}{\beta} (x - \tau) - \cos \frac{2\pi}{\beta} \epsilon_2} \right]. \quad (5.77)$$

Again, we see that this precisely coincides with the expectation value of the $U(1)$ current obtained from the backreacted solution of the in-falling geodesic in (5.60) using the identification (5.75). A similar calculation can also be done for the expectation value of the j_x component, resulting in the holographic result (5.61). Finally, let us evaluate the expectation value of the marginal operator Ψ of dimension $(1, 1)$ in the state (5.68).

$$\begin{aligned} \langle \Psi \rangle_{CFT} &= \text{Tr}(\rho \Psi(x - \tau, x + \tau)), \\ &= \frac{\langle \mathcal{O}^\dagger(w_2, \bar{w}_2) \psi(x - \tau, x + \tau) \mathcal{O}(w_1, \bar{w}_1) \rangle_\beta}{\langle \mathcal{O}^\dagger(w_2, \bar{w}_2) \bar{\mathcal{O}}(w_1, \bar{w}_1) \rangle_\beta}. \end{aligned} \quad (5.78)$$

Evaluating the correlator, by conformally mapping the cylinder to the plane, we obtain

$$\langle \Psi \rangle_{CFT} = -\Delta \left(\frac{2\pi}{\beta} \right)^2 \left[\frac{\sin \frac{2\pi}{\beta} \epsilon_1 \sin \frac{2\pi}{\beta} \epsilon_2}{\left\{ \cosh \frac{2\pi}{\beta} (x + \tau) - \cos \frac{2\pi}{\beta} \epsilon_1 \right\} \left\{ \cosh \frac{2\pi}{\beta} (x - \tau) - \cos \frac{2\pi}{\beta} \epsilon_2 \right\}} \right] \quad (5.79)$$

Comparing with (5.65), we see that this expression for the expectation value of the marginal operator Ψ precisely agrees with that evaluated from the backreacted geometry of an in-falling geodesic upon using the relations in (5.75). In conclusion, we have shown that the spinning in falling particle in the BTZ geometry is dual to a local quench carrying $U(1)$ R-charge corresponding to the angular momentum in the S^3 . In general, the left and right moving pulses of the quench are not symmetric. The quench also carried the expectation value of a marginal operator.

5.3 Quenches dual to the circular string

Let us consider the circular string solution in $AdS_3 \times S^3 \times M$ given by

$$\begin{aligned} t(\sigma^0, \sigma^1) &= \kappa \sigma^0, \quad r(\sigma^0, \sigma^1) = 0, \quad \phi(\sigma^0, \sigma^1) = 0, \\ \psi &= \tan^{-1} \left(\sqrt{\frac{W - qm}{W + qm}} \right) \equiv \psi_0, \quad \phi_1 = \sigma^0 (W + qm) + m\sigma^1, \quad \phi_2 = \sigma^0 (W - qm) - m\sigma^1, \\ X(\sigma^0, \sigma^1)|_M &= x_m = \text{constant}. \end{aligned} \quad (5.80)$$

with $m \in \mathbb{Z}$. Here, we have used the parametrisation (3.6), for the metric of S^3 given in (3.7).

$$\kappa^2 = \omega^2 + m^2, \quad W^2 = w^2 + q^2 m^2. \quad (5.81)$$

The angular momentum and the dispersion relation are given by

$$\begin{aligned} J_1 = J_2 &= \frac{k}{2}(W - qm), \quad J \equiv J_1 + J_2, \\ \Delta &= k\kappa = \sqrt{(J + qkm)^2 + k^2 m^2 (1 - q^2)}. \end{aligned} \quad (5.82)$$

The world sheet couples to the target space metric by the action given in (5.10). We substitute the solution and derive the spacetime stress tensor. To un-clutter the equations, we first define the delta function

$$\hat{\delta} \equiv \frac{\delta(r)\delta(\phi)}{r} \frac{\delta(\psi - \psi_0)\delta(\phi_1 + \phi_2 - \frac{2W}{\kappa}t)}{\sqrt{g_{S^3}}} \frac{\delta^4(X_M - x_M)}{\sqrt{G_M}}. \quad (5.83)$$

Then the stress tensor sourced by the circular string solution for $m \neq 0$ is given by

$$\begin{aligned} T^{t t} &= \frac{\Delta}{2\pi m R} \hat{\delta}, \quad T^{t \phi_1} = \frac{J + 2kqm}{2\pi m R} \hat{\delta}, \\ T^{t \phi_2} &= \frac{J}{2\pi m R} \hat{\delta}, \quad T^{\phi_1 \phi_1} = \frac{(J + 2kqm)^2 - k^2 m^2}{2\pi m R \Delta} \hat{\delta}, \\ T^{\phi_2 \phi_2} &= \frac{J^2 - k^2 m^2}{2\pi m R \Delta} \hat{\delta}, \quad T^{\phi_1 \phi_2} = \frac{J(J + 2kqm) - k^2 m^2}{2\pi m R \Delta} \hat{\delta}. \end{aligned} \quad (5.84)$$

We have to treat the case $m = 0$ for which there is no world sheet spatial dependence, separately. For this case, the delta function would become

$$\hat{\delta} \rightarrow \check{\delta} \equiv \frac{\delta(r)\delta(\phi)}{r} \frac{\delta(\psi - \psi_0)\delta(\phi_1 - \frac{W}{\kappa}t)\delta(\phi_2 - \frac{W}{\kappa}t)}{\sqrt{g_{S^3}}} \frac{\delta^4(X_M - x_M)}{\sqrt{G_M}}. \quad (5.85)$$

The strength of all the stress tensor components then becomes $\frac{\Delta}{R}$, which is the expected situation for a geodesic. Compactifying on $S^3 \times M$, we obtain the following sources. The Einstein equations on the metric in 3d gets a source term given by the stress tensor

$$T_{\mu\nu} = \frac{\Delta}{R} \frac{\delta(r)\delta(\phi)}{r}. \quad (5.86)$$

Note that we have integrated the stress tensor in 10 dimensions given in (5.84) in all the compact directions. The angle ϕ_1 needs to be integrated from 0 to $2\pi m$, since the circular string is wrapped m times along ϕ_1 . The metric fluctuations with one of the components in ϕ_1 or ϕ_2 results in 2 $U(1)$, Chern-Simons gauge fields $A_\mu^{\phi_1}, A_\mu^{\phi_2}$ respectively. They are sourced by the following current density in $3d$

$$J_{\phi_1}^t = \frac{(J + 2kqm)}{R} \frac{\delta(r)\delta(\phi)}{r}, \quad J_{\phi_2}^t = \frac{J}{R} \frac{\delta(r)\delta(\phi)}{r}. \quad (5.87)$$

Finally there are three scalars in $3d$ labelled as ψ_1, ψ_2, ψ_3 which are sourced by

$$\begin{aligned} J_{\psi_1} &= \frac{(J + 2kqm)^2 - k^2 m^2}{R\Delta} \frac{\delta(r)\delta(\phi)}{r}, \\ J_{\psi_2} &= \frac{J^2 - k^2 m^2}{R\Delta} \frac{\delta(r)\delta(\phi)}{r}, \\ J_{\psi_3} &= \frac{J(J + 2kqm) - k^2 m^2}{R\Delta} \frac{\delta(r)\delta(\phi)}{r}. \end{aligned} \quad (5.88)$$

At least one of the scalars is massless since, as we have argued earlier in section 5.1, the dilaton couples to the scalar components of the stress tensor. We would have to study the compactification in more detail to figure out the mass of the other scalars. Observe that we can take the winding number $m = 0$ and use $\Delta = J$ to obtain the sources in the compactified theory for the case of the circular string without world sheet spatial dependence. We can now proceed to find the backreacted solution just as we have done for the geodesic in section 5.1. The difference would be that there is an additional gauge field, and 2 additional scalars in the bulk, which have a non-trivial solution. This implies that the operator in the CFT \mathcal{O} has an additional R-charge and there are 2 additional operators with non-trivial 3 point functions with \mathcal{O} . Finally, we can perform the coordinate transformation in (2.43) to the back reacted solution to the in-falling circular string in BTZ and demonstrate that these are dual to quenches that carry R charge and expectation values of scalars. We will not carry out this analysis, but the same procedure done for the geodesic in section 5.2 can be repeated here. This will result in the demonstration that the in-falling circular strings are quenches in the thermal CFT. It is clear that the backreacted metric is identical to that of the in-falling geodesic, since comparing (5.16) and (5.86) we see that the source for the metric corrections is identical. Finally, we remark that the backreacted solution for the giant magnon solution can be treated following the same approach as for the circular string. It is clear from our analysis of the circular string and that of the geodesic, the in-falling Magnon in the BTZ geometry will be a quench sourcing energy density, R-charges as well as certain scalar expectation values in the thermal CFT.

6 Conclusions

We have studied the spectrum of string states that fall into the horizon of the $BTZ \times S^3 \times M$ geometry and their dual description in the thermal field theory. The states consist of geodesics, circular strings, giant magnons, and plane waves. These solutions were obtained by utilising the map which relates the time-like geodesic at the origin of $AdS_3 \times S^3 \times M$

and spinning on S^3 to the in-falling particle in the BTZ geometry. This map was used to zoom into a geometry in the BTZ black hole for which the plane wave spectrum is identical to that of AdS_3 . We have also shown that the dual description of the classical solutions in-falling into the BTZ horizon are generalised local quenches in the thermal CFT. These quenches are not symmetric on the left and right light cones when the classical solution has velocity along the boundary of the BTZ background; they carry R-charges and expectation values of other operators in the theory.

Early studies of strings in BTZ explored the fact that it is an orbifold of AdS_3 and derived properties of the spectrum with an emphasis on twisted states and integrability [6, 10, 11, 36–44]. It will be interesting to re-examine these works in the light of the fact that there are states that fall into the horizon of the BTZ and identify these states from the general analysis.

The analysis done in this paper can be generalised for hyperbolic black holes in higher dimensions. This is because there is a map that takes the AdS_d with $d > 3$ to the hyperbolic black hole or AdS_d Rindler [13]. Therefore, circular strings and giant magnon solutions in $AdS_5 \times S^5$ or $AdS_4 \times S^7$ can be related to solutions falling into the AdS_d Rindler space time. Following our analysis further would lead to a dual description of these solutions in the thermal CFT on the hyperbolic cylinder $S^1 \times H_{d-2}$. It would be interesting to make this more explicit and explore other possible deformations of the map (2.43) as we have done for the case of AdS_3 .

A by-product of our study was the observation of more general local quenches in thermal CFT. The important aspect of these quenches is that the left and right pulses on the light cone are not symmetric. They also carry R-charges and expectation values of other operators. It will be interesting to study these quenches in more detail, especially the evolution of entanglement entropy on the lines of [29]. Since these quenches carry R-charges, it is possible that notions of symmetry resolved entanglement [45] might play a role.

Acknowledgments

We thank Rajesh Gopakumar for discussions at various stages of this project, whose questions led us to study the spacetime charges of the in-falling states in BTZ. Rahul Metya would like to thank Ritwick Kumar Ghosh for stimulating discussions. J.R.D thanks S. Prem Kumar and Suvajit Majumder for an enjoyable collaboration during the difficult Covid times in which asymmetric quenches were first found in the BTZ background.

A Penrose limit of Schwarzschild black hole in $AdS_5 \times S^5$

Consider the Schwarzschild black hole in $AdS_5 \times S_5$, the metric is given in

$$R^{-2}ds^2 = - \left(r^2 + 1 - \frac{r_0^2}{r^2} \right) dt^2 + \frac{dr^2}{\left(r^2 + 1 - \frac{r_0^2}{r^2} \right)} + r^2 (d\phi^2 + \sin^2 \phi d\Omega^2) + d\psi^2 + \sin^2 \psi d\Omega_4^2 \quad (\text{A.1})$$

Consider the case of a null geodesic carrying angular momentum along ϕ , one of the circles in the AdS_5 directions. The trajectory of this geodesic is given in equation (4.2). We now perform the usual steps to take the Penrose limit along this geodesic. We first make the change of coordinates from (t, r, ϕ) to (λ, ξ, θ) such that

$$g_{\lambda\lambda} = g_{\lambda\theta} = 0, \quad \text{and} \quad g_{\lambda\xi} = 1 \quad (\text{A.2})$$

In this new coordinate system, λ is the usual affine parameter that we have used before to write down the geodesic, and ξ and ψ are the integration constants. We choose the integration constant in such a way that the above conditions, i.e., equation (A.2), are met. So, one of the ways to choose the new coordinates is the following

$$t(\lambda, \xi, \theta) = \int_0^\lambda \dot{t} d\lambda' - \frac{\xi}{E} + J\theta, \quad r(\lambda, \xi, \theta) = \int_0^\lambda \dot{r} d\lambda', \quad \phi(\lambda, \xi, \theta) = E\theta + \int_0^\lambda \dot{\phi} d\lambda' \quad (\text{A.3})$$

We substitute this transformation in A.1 and get

$$\begin{aligned} R^{-2}ds^2 &= \left(-a_0\dot{t}^2 + a_0^{-1}\dot{r}^2 + r^2\dot{\phi}^2\right)d\lambda^2 - a_0E^{-2}d\xi^2 + (r^2E^2 - a_0J^2)d\theta^2 + (a_0E^{-1}\dot{t})2d\lambda d\xi \\ &\quad + (-a_0J\dot{t} + JE)2d\lambda d\theta + (a_0JE^{-1})2d\xi d\theta + r^2\sin^2\phi d\Omega_2^2 + ds^2(S^5) \\ &= 2d\lambda d\xi - a_0E^{-2}d\xi^2 + (r^2E^2 - J^2a_0)d\theta^2 + Ja_0E^{-1}2d\xi d\theta + r^2\sin^2\phi d\Omega_2^2 + ds^2(S^5) \end{aligned}$$

Here we have redefined: $a_0 \equiv \left(r^2 + 1 - \frac{r_0^2}{r^2}\right)$. Now, we perform the following rescaling,

$$\lambda \rightarrow \lambda, \quad \xi \rightarrow \frac{\xi}{R^2}, \quad \theta \rightarrow \frac{\theta}{R}, \quad \psi \rightarrow \frac{\psi}{R} \quad (\text{A.4})$$

and expanding the metric in the large R limit, we obtain

$$ds^2 = 2d\lambda d\xi + (r^2E^2 - J^2a_0)d\theta^2 + r^2\sin^2\left(\int_0^\lambda \frac{J}{r^2} d\lambda'\right)ds^2(\mathbb{R}^2) + ds^2(\mathbb{R}^5) \quad (\text{A.5})$$

$$= 2d\lambda d\xi + \sum_{i=1}^8 (C_i dy^i)^2 \quad (\text{A.6})$$

The above metric, equation (A.5), is the plane wave metric in the Rosen coordinate. We go to Brinkmann coordinates by the following coordinate transformation

$$\lambda = x^+, \quad \xi = x^- + \frac{1}{2} \sum_i \frac{1}{C_i} \left(\frac{\partial C_i}{\partial x^+} \right) x^i x^i, \quad y^i = C_i^{-1} x^i \quad (\text{A.7})$$

Then the metric becomes

$$\begin{aligned} ds^2 &= 2dx^+ dx^- + \left[\sum_i \frac{C''(x^+)}{C_i} x^i x^i \right] (dx^+)^2 + \sum_i dx^i dx^i \\ &= 2dx^+ dx^- + \sum_i (M_{ii} x^i x^i) (dx^+)^2 + \sum_i dx^i dx^i \end{aligned}$$

To evaluate the matrix M , we first write the derivative with respect to λ in terms of derivative with respect to r as,

$$\frac{d^2}{d\lambda^2} = \frac{d}{d\lambda} \left(\dot{r} \frac{d}{dr} \right) = \dot{r}^2 \frac{d^2}{dr^2} + \dot{r} \left(\frac{d\dot{r}}{dr} \right) \frac{d}{dr} \quad (\text{A.8})$$

Using the above relation, we compute all the components of the M matrix

$$\begin{aligned} M_{11} &= r^{-1} \frac{d}{dr} \left[\dot{r} \frac{d}{dr} (\dot{r}r) \right] = \frac{4J^2r_0^2}{r^6}; \quad M_{44} = \dots = M_{88} = 0 \\ M_{22} = M_{33} &= \frac{\dot{r}}{r \sin \left(\int \frac{J}{r^2} du \right)} \frac{d}{dr} \left[\dot{r} \frac{d}{dr} \left\{ r \sin \left(\int \frac{J}{r^2} du \right) \right\} \right] = -\frac{2J^2r_0^2}{r^6} \end{aligned} \quad (\text{A.9})$$

This results in the following pp wave metric in Brinkmann coordinates

$$ds^2 = 2dx^+dx^- + \left[\frac{4J^2r_0^2}{r^6}x_1^2 - \frac{2J^2r_0^2}{r^6}(x_2^2 + x_3^2) \right] (dx^+)^2 + \sum_{i=1}^3 dx_i^2 + \sum_{i=1}^5 dy_i^2 \quad (\text{A.10})$$

Now we examine the situation in which the null geodesic has angular momenta along one of the circles of S^5 . This case was addressed in [14] with a slightly different metric for the AdS_5 Schwarzschild black hole. The trajectory of this geodesic is already given by the equation (4.4). As before, we follow similar steps to take the Penrose Limit. We begin with a change of coordinate from (t, r, ψ) to (λ, ξ, χ) which is given by

$$t(\lambda, \xi, \chi) = \int_0^\lambda \dot{t} d\lambda' - \frac{\xi}{E} + J\chi, \quad r(\lambda, \xi, \chi) = \int_0^\lambda \dot{r} d\lambda', \quad \psi(\lambda, \xi, \chi) = E\chi + J\lambda. \quad (\text{A.11})$$

Substituting this coordinate transformation in the metric (A.1), we perform the following rescaling

$$\lambda \rightarrow \lambda, \quad \xi \rightarrow \frac{\xi}{R^2}, \quad \chi \rightarrow \frac{\chi}{R}, \quad \phi \rightarrow \frac{\phi}{R}. \quad (\text{A.12})$$

Now expanding the metric in the large R limit, we obtain the pp wave in the Rosen Coordinate

$$ds^2 = 2d\lambda d\xi + (E^2 - J^2a_0) d\theta^2 + r^2 ds^2(\mathbb{R}^3) + \sin^2(J\lambda) ds^2(\mathbb{R}^4). \quad (\text{A.13})$$

Next, we go to the Brinkmann Coordinate and calculate the mass matrix

$$\begin{aligned} \tilde{M}_{11} &= \left[E^2 - J^2 \left(r^2 + 1 - \frac{r_0^2}{r^2} \right) \right]^{-\frac{1}{2}} \frac{d^2}{d\lambda^2} \left(\sqrt{1 - J^2 \left(r^2 + 1 - \frac{r_0^2}{r^2} \right)} \right) \\ &= \frac{d}{dr} \left(\dot{r} \frac{d}{dr} (\dot{r}) \right) = -J^2 \left(1 - \frac{3r_0^4}{r^4} \right) \end{aligned} \quad (\text{A.14})$$

$$\tilde{M}_{22} = \frac{1}{r} \frac{d^2}{d\lambda^2}(r) = \frac{1}{r} \left[\dot{r}^2 \frac{d^2}{dr^2} + \dot{r} \left(\frac{d\dot{r}}{dr} \right) \frac{d}{dr} \right](r) = \dot{r} \left(\frac{d\dot{r}}{dr} \right)^2 = -J^2 \left(1 + \frac{r_0^4}{r^4} \right) = \tilde{M}_{33} = \tilde{M}_{44} \quad (\text{A.15})$$

$$\tilde{M}_{55} = \frac{1}{\sin(J\lambda)} \frac{d^2}{d\lambda^2} (\sin(J\lambda)) = -J^2 = \tilde{M}_{66} = \tilde{M}_{77} = \tilde{M}_{88}. \quad (\text{A.16})$$

Finally, we obtain

$$ds^2 = 2dx^+dx^- - J^2 \left[\left(1 - \frac{3r_0^4}{r^4} \right) x_1^2 + \left(1 + \frac{r_0^4}{r^4} \right) z_3^2 + z_4^2 \right] (dx^+)^2 + dz_3^2 + dz_4^2 \quad (\text{A.17})$$

where z_3 parametrizes \mathbb{R}^3 and z_4 parametrizes \mathbb{R}^4 . This solution is supported by five-form flux, which is given by

$$F_5 = R^4 [\text{vol}(AdS_5) + \text{vol}(S^5)] \quad (\text{A.18})$$

where

$$\text{Vol}(AdS_5) = r^3 dt \wedge dr \wedge \text{Vol}(S^3), \quad \text{Vol}(S^5) = \sin^4 \psi \, d\psi \wedge \text{Vol}(S^4) \quad (\text{A.19})$$

Substituting the coordinates transformation given in (A.11) in the above equation and taking the large R limit, we obtain

$$\begin{aligned} \text{Vol}(AdS_5) &= R^4 r^3 dt \wedge dr \wedge \text{Vol}(S^3) \\ &= R^4 r^3 \left(t_\lambda d\lambda - \frac{d\xi}{E} + J d\phi \right) \wedge (r_\lambda d\lambda) \wedge \text{Vol}(S^3) \\ &= R^4 r^3 r_\lambda \left[-\frac{d\xi}{E} \wedge d\lambda \wedge \text{Vol}(S^3) + J d\phi \wedge d\lambda \wedge \text{Vol}(S^3) \right] \\ &= J d\phi \wedge (r_\lambda d\lambda) \wedge (r^3 \text{Vol}(\mathbb{R}^3)) \\ \text{Vol}(S^5) &= R^4 \sin^4 \psi \, d\psi \wedge \text{Vol}(S^4) \\ &= R^4 \sin^4 (J\lambda + E\phi) \{ J d\lambda + E d\phi \} \wedge \text{Vol}(S^4) \\ &= J d\lambda \wedge \sin^4 (J\lambda) \text{Vol}(\mathbb{R}^4) \end{aligned} \quad (\text{A.20})$$

Going to the Brinkmann coordinates, we obtain

$$F_5 = J dx^+ \wedge (dx_1 \wedge dx_2 \wedge dx_3 \wedge dx_4 + dx_5 \wedge dx_6 \wedge dx_7 \wedge dx_8) \quad (\text{A.21})$$

References

- [1] M. Banados, C. Teitelboim and J. Zanelli, *The Black hole in three-dimensional space-time*, *Phys. Rev. Lett.* **69** (1992) 1849 [[hep-th/9204099](#)].
- [2] M. Banados, M. Henneaux, C. Teitelboim and J. Zanelli, *Geometry of the (2+1) black hole*, *Phys. Rev. D* **48** (1993) 1506 [[gr-qc/9302012](#)].
- [3] J.M. Maldacena and A. Strominger, *AdS(3) black holes and a stringy exclusion principle*, *JHEP* **12** (1998) 005 [[hep-th/9804085](#)].
- [4] S. Datta and J.R. David, *Higher Spin Quasinormal Modes and One-Loop Determinants in the BTZ black Hole*, *JHEP* **03** (2012) 079 [[1112.4619](#)].
- [5] S. Datta and J.R. David, *Higher spin fermions in the BTZ black hole*, *JHEP* **07** (2012) 079 [[1202.5831](#)].
- [6] M. Natsuume and Y. Satoh, *String theory on three-dimensional black holes*, *Int. J. Mod. Phys. A* **13** (1998) 1229 [[hep-th/9611041](#)].

[7] Y. Satoh, *Ghost - free and modular invariant spectra of a string in $SL(2,R)$ and three-dimensional black hole geometry*, *Nucl. Phys. B* **513** (1998) 213 [[hep-th/9705208](#)].

[8] J.M. Maldacena and H. Ooguri, *Strings in $AdS(3)$ and $SL(2,R)$ WZW model 1.: The Spectrum*, *J. Math. Phys.* **42** (2001) 2929 [[hep-th/0001053](#)].

[9] J.M. Maldacena, H. Ooguri and J. Son, *Strings in $AdS(3)$ and the $SL(2,R)$ WZW model. Part 2. Euclidean black hole*, *J. Math. Phys.* **42** (2001) 2961 [[hep-th/0005183](#)].

[10] S. Hemming and E. Keski-Vakkuri, *The Spectrum of strings on BTZ black holes and spectral flow in the $SL(2,R)$ WZW model*, *Nucl. Phys. B* **626** (2002) 363 [[hep-th/0110252](#)].

[11] S. Hemming, E. Keski-Vakkuri and P. Kraus, *Strings in the extended BTZ space-time*, *JHEP* **10** (2002) 006 [[hep-th/0208003](#)].

[12] D.E. Berenstein, J.M. Maldacena and H.S. Nastase, *Strings in flat space and pp waves from $N=4$ superYang-Mills*, *JHEP* **04** (2002) 013 [[hep-th/0202021](#)].

[13] H. Casini, M. Huerta and R.C. Myers, *Towards a derivation of holographic entanglement entropy*, *JHEP* **05** (2011) 036 [[1102.0440](#)].

[14] L.A. Pando Zayas and J. Sonnenschein, *On Penrose limits and gauge theories*, *JHEP* **05** (2002) 010 [[hep-th/0202186](#)].

[15] P. Caputa, J. Simón, A. Štikonas and T. Takayanagi, *Quantum Entanglement of Localized Excited States at Finite Temperature*, *JHEP* **01** (2015) 102 [[1410.2287](#)].

[16] S. Elitzur, O. Feinerman, A. Giveon and D. Tsabar, *String theory on $AdS_3 \times S^3 \times S^3 \times S^1$* , *Phys. Lett. B* **449** (1999) 180 [[hep-th/9811245](#)].

[17] B. Hoare, A. Stepanchuk and A.A. Tseytlin, *Giant magnon solution and dispersion relation in string theory in $AdS_3 \times S^3 \times T^4$ with mixed flux*, *Nucl. Phys. B* **879** (2014) 318 [[1311.1794](#)].

[18] H.-Y. Chen, N. Dorey and K. Okamura, *Dyonic giant magnons*, *Journal of High Energy Physics* **2006** (2006) 024–024.

[19] D.M. Hofman and J. Maldacena, *Giant magnons*, *Journal of Physics A: Mathematical and General* **39** (2006) 13095–13117.

[20] M. Blau, M. Borunda, M. O’Loughlin and G. Papadopoulos, *Penrose limits and space-time singularities*, *Class. Quant. Grav.* **21** (2004) L43 [[hep-th/0312029](#)].

[21] M. Blau, M. Borunda, M. O’Loughlin and G. Papadopoulos, *The Universality of Penrose limits near space-time singularities*, *JHEP* **07** (2004) 068 [[hep-th/0403252](#)].

[22] M. Blau, J.M. Figueroa-O’Farrill and G. Papadopoulos, *Penrose limits, supergravity and brane dynamics*, *Class. Quant. Grav.* **19** (2002) 4753 [[hep-th/0202111](#)].

[23] A. Dei, M.R. Gaberdiel and A. Sfondrini, *The plane-wave limit of $AdS_3 \times S^3 \times S^3 \times S^1$* , *JHEP* **08** (2018) 097 [[1805.09154](#)].

[24] C.T. Asplund and S.G. Avery, *Evolution of Entanglement Entropy in the D1-D5 Brane System*, *Phys. Rev. D* **84** (2011) 124053 [[1108.2510](#)].

[25] M. Nozaki, T. Numasawa and T. Takayanagi, *Holographic Local Quenches and Entanglement Density*, *JHEP* **05** (2013) 080 [[1302.5703](#)].

[26] M. Nozaki, T. Numasawa and T. Takayanagi, *Quantum Entanglement of Local Operators in Conformal Field Theories*, *Phys. Rev. Lett.* **112** (2014) 111602 [[1401.0539](#)].

[27] P. Caputa, M. Nozaki and T. Takayanagi, *Entanglement of local operators in large- N conformal field theories*, *PTEP* **2014** (2014) 093B06 [[1405.5946](#)].

[28] C.T. Asplund, A. Bernamonti, F. Galli and T. Hartman, *Holographic Entanglement Entropy from 2d CFT: Heavy States and Local Quenches*, *JHEP* **02** (2015) 171 [[1410.1392](#)].

[29] J.R. David, S. Khetrapal and S.P. Kumar, *Universal corrections to entanglement entropy of local quantum quenches*, *JHEP* **08** (2016) 127 [[1605.05987](#)].

[30] J. de Boer, *Six-dimensional supergravity on $S^3 \times AdS_3$ and 2-D conformal field theory*, *Nucl. Phys. B* **548** (1999) 139 [[hep-th/9806104](#)].

[31] J.R. David, *Anti-de Sitter gravity associated with the supergroup $SU(1, 1|2) \times SU(1, 1|2)$* , *Mod. Phys. Lett. A* **14** (1999) 1143 [[hep-th/9904068](#)].

[32] N.S. Deger, H. Samtleben, O. Sarioglu and D. Van den Bleeken, *A supersymmetric reduction on the three-sphere*, *Nucl. Phys. B* **890** (2014) 350 [[1410.7168](#)].

[33] H. Samtleben and Ö. Sarioglu, *Consistent S^3 reductions of six-dimensional supergravity*, *Phys. Rev. D* **100** (2019) 086002 [[1907.08413](#)].

[34] J.R. David, G. Mandal and S.R. Wadia, *Microscopic formulation of black holes in string theory*, *Phys. Rept.* **369** (2002) 549 [[hep-th/0203048](#)].

[35] P. Kraus, *Lectures on black holes and the AdS_3/CFT_2 correspondence*, *Lect. Notes Phys.* **755** (2008) 193 [[hep-th/0609074](#)].

[36] J. Troost, *Winding strings and $AdS(3)$ black holes*, *JHEP* **09** (2002) 041 [[hep-th/0206118](#)].

[37] M. Rangamani and S.F. Ross, *Winding tachyons in BTZ*, *Phys. Rev. D* **77** (2008) 026010 [[0706.0663](#)].

[38] M. Berkooz, Z. Komargodski and D. Reichmann, *Thermal $AdS(3)$, BTZ and competing winding modes condensation*, *JHEP* **12** (2007) 020 [[0706.0610](#)].

[39] J.R. David and A. Sadhukhan, *Classical integrability in the BTZ black hole*, *JHEP* **08** (2011) 079 [[1105.0480](#)].

[40] J.R. David, C. Kalousios and A. Sadhukhan, *Generating string solutions in BTZ*, *JHEP* **02** (2013) 013 [[1211.5382](#)].

[41] T.G. Mertens, *Hagedorn String Thermodynamics in Curved Spacetimes and near Black Hole Horizons*, Ph.D. thesis, Gent U., 2015. [1506.07798](#).

[42] S.K. Ashok and J. Troost, *Twisted strings in three-dimensional black holes*, *Eur. Phys. J. C* **82** (2022) 913 [[2112.08784](#)].

[43] O.V. Nippanikar, A. Sharma and K.P. Yogendran, *The BTZ black hole spectrum and partition function*, [2112.11253](#).

[44] S.K. Ashok and J. Troost, *Long strings and quasinormal winding modes*, *JHEP* **09** (2022) 172 [[2207.05361](#)].

[45] S. Zhao, C. Northe and R. Meyer, *Symmetry-resolved entanglement in AdS_3/CFT_2 coupled to $U(1)$ Chern-Simons theory*, *JHEP* **07** (2021) 030 [[2012.11274](#)].